On a hybrid updating method for modeling vibroacoustic behaviors of composite panels

Yahya Allahtavakoli, Mohamed Ichchou, Catherine Marquis-Favre, Nacer Hamzaoui

▶ **To cite this version:**

Yahya Allahtavakoli, Mohamed Ichchou, Catherine Marquis-Favre, Nacer Hamzaoui. On a hybrid updating method for modeling vibroacoustic behaviors of composite panels. Journal of Sound and Vibration, 2023, 565, pp.117902. 10.1016/j.jsv.2023.117902 . hal-04164620

HAL Id: hal-04164620
https://hal.science/hal-04164620v1

Submitted on 14 Nov 2024

HAL is a multi-disciplinary open access archive for the deposit and dissemination of scientific research documents, whether they are published or not. The documents may come from teaching and research institutions in France or abroad, or from public or private research centers.

L'archive ouverte pluridisciplinaire **HAL**, est destinée au dépôt et à la diffusion de documents scientifiques de niveau recherche, publiés ou non, émanant des établissements d'enseignement et de recherche français ou étrangers, des laboratoires publics ou privés.

On a hybrid updating method for modeling vibroacoustic behaviors of composite panels

Y. AllahTavakoli[a,b,c], M.N. Ichchou[b], C. Marquis-Favre[a], and N. Hamzaoui[c]

[a] *Univ Lyon, ENTPE, Ecole Centrale de Lyon, CNRS, LTDS, UMR5513, 69518 Vaulx-en-Velin, France, (Email: yahya.allahtavakoli@entpe.fr)*

[b] *Univ Lyon, Ecole Centrale de Lyon, CNRS, ENTPE, LTDS, UMR5513, 69130 Ecully, France*

[c] *Univ Lyon, INSA-Lyon, Laboratoire Vibrations Acoustique, LVA EA677, F-69621, Villeurbanne, France*

Abstract

Composite panels, by virtue of their outstanding mechanical properties, have found various applications in different sectors like aerospace and transportation. Under certain assumptions like Kirchhoff–Love and Mead-Markus hypotheses, certain high-order differential equations can be used for vibroacoustic modeling of composite panels. However, for accurate modeling, updating parameters is an essential stage. Herein, we aim to theoretically and experimentally review this stage. For this purpose, a hybrid updating method is proposed, incorporating hierarchical functions, inhomogeneous wave correlation approach, and least squares optimizations. Then various laboratory measurements, including Laser Doppler Vibrometry measurements as well as sound pressure levels, are analyzed. The measurements were performed for a thick composite (sandwich) panel, and a thin composite (laminate) one, along with two isotropic (steel and aluminum) plates for additional validation. The experiments indicate the ability of the hybrid approach to adjust parameters and precisely model vibroacoustic behaviors of the panels. Furthermore, the proposed hybrid

method can be used in studies whose goal is accurate vibroacoustic modeling for psychoacoustic issues and perceptual validations, which is also one of the future targets of this research.

Keywords— Updating; parameter identification; vibroacoustic; composite sandwich; composite laminate, orthotropic panels

1 Introduction

Nowadays in different sectors of high-tech industries like aerospace and high-speed transportation, we can find an accelerating trend in the usage of composite materials due to their outstanding mechanical properties. Composite materials have found a widespread acceptance in aeronautic and space studies during recent decades (e.g. see Giurgiutiu (2015)), and today, new airframes mainly consist of composites, such as Boeing 787 Dreamliner and Airbus A350 XWB in which composites possess 80% participation by volume (e.g. see Mrazova (2013); Giurgiutiu (2015)). Also, in the transportation industry, there are other advanced applications, where these materials have found an undeniable key role in manufacturing high-speed trains, and they possess many advantages like lighter weight, acceptable tensile strength, enhanced stability, corrosion resistance, sound baffling, and design flexibility (e.g. see Fan and Njuguna (2016)).

The optimal design of composite structures is a burning issue (e.g, see Jones (2018)), and having a precise prediction about their vibroacoustic behavior is an essential stage for design optimization. The uncertainty remaining in numerical models and their parameters is the major barrier to precisely modeling the structure dynamics (e.g. see Friswell and Mottershead (1995)). Hence, model and parameter updating will be essential to reduce such uncertainty remaining in the models, and their parameters (Friswell and Mottershead (1995)). The purpose of parameter updating is to present physical meaning to a deficient model from real experiments where the model suffers from a lack of precise knowledge about mechanical parameters, boundary conditions, and component connections (Mottershead and Friswell (1993)). Although in recent decades, many studies can be found in this regard, this issue is still of great interest to many researchers for either updating or identifying parameters in different case studies (e.g. see Girardi et al. (2021); Standoli et al. (2021); Chengwei et al. (2022)).
In the research conducted in the nineties, one can come across useful studies for

reviewing advanced methods of updating (e.g. see Friswell (1990), Mottershead and Friswell (1993) and Humbert (1999)). These studies were then followed by studies on parameter identification, model updating, damage identification, and health monitoring in the context of different mechanical behaviors at the beginning of the 21st century (Farrar et al. (2001); Sinha et al. (2002); Carden and Fanning (2004); Živanović et al. (2005); Kerschen et al. (2006)). Afterward, other studies like Chen et al. (2006) performed analyses for investigating model and data uncertainties in structural dynamics with a case study of composite sandwich panels. Chen et al. (2006) dealt with the experimental identification, model updating, and validation of a non-parametric probabilistic method.

Meanwhile, parameter identification was another important issue in the parameter updating associated with composite sandwich panels. For instance, for the parameter identification, following Berthaut et al. (2005) which set the bases of inhomogeneous wave correlation method (IWC), Ichchou et al. (2008) proposed an approach and applied it to one and two-dimensional sandwich structures with honeycomb cores. Their approach is founded on the k-space characteristics of measured or simulated data and it starts from the spatially distributed fields of a vibrating structure for identifying the complete dispersion curve. The method of Ichchou et al. (2008) uses a harmonic field as the primary input, and then the correlation between this harmonic field and an inhomogeneous wave is calculated, leading to a wavenumber-dependent objective function, called Inhomogeneous Wave Correlation (IWC). Also, the approach includes an inverse technique for the optimization of the correlation index. Ichchou et al. (2008) successfully compared the technique with another wavenumber identification tool proposed by McDaniel et al. (2000) and McDaniel and Shepard Jr (2000). Finally, in this research, parameter identification was attained via a least square algorithm, where a sandwich honeycomb was examined via the proposed method, and the results were successfully validated by an analytical model of Nilsson and Nilsson (2002). Afterward, the IWC approach was also followed by other researchers in their parameter identification studies like Chronopoulos et al. (2013), Cherif et al. (2015), and Van Belle et al. (2017).

Besides, nowadays by virtue of high-tech laser vibrometers and digital cameras, we are able to carry out the parameter identification and updating via using full-field vibration data. The increasing usage of these technologies in modal analysis has made full-field measurement of vibration mode shapes available (Mottershead et al. (2011)). Wang et al. (2011) presented a study on model updating from full-field vibration measurement using digital image correlation. This study shows

how such a comparison of structural responses between predictions and full-field vibration measurements is an essential step in model updating.

In recent years, we can also come across other different studies for updating, optimizing, and identifying mechanical parameters of composite panels. For instance, Esfandiari (2014) proposed a model updating algorithm for estimating structural parameters at the element level using frequency domain representation of the strain data. Also, Tsai et al. (2015) propounded the optimization approach that could optimize material properties of a composite panel for a sound transmission problem. Wang et al. (2017) proposed a model updating method based on acceleration frequency response function, and applied a Kriging model to structural acceleration FRF-based model updating. Also, Cuadrado et al. (2019) provided an approach for the model updating of uncertain parameters of carbon/epoxy composite plates from experimental modal data.
Furthermore, along with the above-mentioned studies, another type of updating method has emerged in recent years, which attempts to employ artificial intelligence and machine learning techniques for updating parameters and models. For example, Hwang and He (2006) proposed an adaptive real-parameter simulated annealing genetic algorithm incorporated with natural frequency error function to estimate elastic properties of composite materials. Also, De Albuquerque et al. (2010) assessed delamination damages on composite plates using an Artificial Neural Network for the radiographic image analysis. Katunin and Przystałka (2014) performed a damage assessment on composite plates using fractional wavelet transform of modal shapes with an optimized selection of spatial wavelets. Petrone and Meruane (2017) used an inverse modeling method based on a parallel genetic algorithm for updating mechanical properties throughout a composite panel in order to get a good numerical-experimental correlation. Tam et al. (2019) proposed an identification approach for isotropic and composite panels, known as, the two-stage meta-heuristic hybrid GA-ACO-PSO optimization method that uses the natural frequency error function, and FRF error function in its first and second stages, respectively. Also, Khatir et al. (2021) proposed another two-stage approach to study damage detection, localization, and quantification in Functionally Graded Material (FGM) plate structures.

The integration of various methods to suggest a hybrid approach comes with certain limitations such as challenges related to compatibility between the methods, heightened complexity for users, and the requirement for meticulous assessments. However, these limitations can be largely addressed through the implementation of a specific structure, clear formulations and procedures, and detailed

experimental evaluations. The main advantage of a hybrid method is the utilization of the proven capabilities of previously established methods and its progressive implementation, allowing for the controlled evaluation and enhancement of the updated parameters and model at each stage. Herein, continuing the abovementioned studies, the proposed hybrid approach is founded on concepts of Hierarchical functions, IWC approach, and least squares optimizations, and finally, its abilities are successfully examined in laboratory experiments. Such validated abilities of the proposed method for calculations up to high frequencies, normally not considered in classical simulations, will also be capable of presenting accurate modeling from a perceptual point of view in future psychoacoustic studies, which is one of the future goals of this research, too. Herein, the originality of the proposed hybrid approach owes much to the analytical formulations of the problems, using the capabilities of the IWC technique during updating procedures, and completing the procedures with the total least square optimization, while the ground-truth laboratory measurements accompany and control the procedures in all the steps. The Hierarchical functions have facilitated the advantage of the hybrid method in analyzing the problem analytically and preparing it for optimizations. Additionally, the IWC approach has empowered the parameter identification and control of initial values for the mechanical parameters of the composite panels. Lastly, the utilization of the least squares methods has enhanced the optimization capabilities of the hybrid approach.
Herein, the presentation is as follows: Section 2 presents the definitions and main theoretical concepts of the problems. Section 3 is devoted to the methodology. The hybrid approach adapted for updating parameters is discussed in this Section. Then Section 4 presents laboratory experiments performed for required validations, and also it presents the required discussions corresponding to experimental results. Finally, Section5 ends this paper with concluding remarks.

2 Vibration of composite panels

In this Section, governing partial differential equations (PDEs), called 6^{th} and 4^{th} order problems, which are able to model the vibration behavior of different composite panels, are discussed in detail.

2.1 6^{th} order problem

The 6^{th} order problem refers to a sixth-order PDE for the vibroacoustic modeling of composite sandwich panels, which accounts for various factors including transverse shear deformation, normal deformation, and bending moments to accurately predict the response to external loads. This problem was originally proposed by Mead and Markus (1969) and subsequently developed further by other researchers such as Narayanan and Shanbhag (1981, 1982). Today, the applications of this model can be found in vibroacoustic studies of composite panels and beams. For instance, Alvelid (2013) developed the 6th order problem for a three-layer sandwich beam with a viscoelastic layer in the middle. In this study, the problem was solved in the case of a cantilever sandwich beam, and the results were compared with Finite Element Method (FEM) calculations. Also, Droz et al. (2017) derived analytical expressions for the equivalent bending and shear parameters by relating them to the transition frequency and the maximal group velocity, and this study employed the 6th order problem to investigate the group velocity. In a recent study by Kohsaka et al. (2021), the vibration characteristics of a sandwich beam with a lattice core were investigated using an analytical approach as well as finite element analyses. The analytical approach focused on solving the 6th order problem to express the motion in terms of the transverse displacement.
In practice, since the shear effects are not usually negligible for composite sandwich plates, the flexural vibrating motions of such panels are usually expected to satisfy high-order problems like the 6^{th} order problem that can demonstrate the flexural motion in a spatial-time domain. For this purpose, one considers a vibrating composite sandwich panel with a $a \times b$ rectangular shape (see Figure1). The panel is excited by an external point force $q(t,x,y) = q(t)\delta(x-x_0)\delta(y-y_0)$ exerted at point (x_0, y_0). Then the 6^{th} order problem is introduced as follows (Mead and Markus (1969); Narayanan and Shanbhag (1981, 1982)):

$$D_t\nabla^6 w - D_t\acute{g}(1+Y)\nabla^4 w + M\frac{\partial^2}{\partial t^2}(\nabla^2 w - \acute{g}w) = \nabla^2 q - \acute{g}q \tag{1}$$

where $w(x,y,t)$ is the transverse displacement, $\nabla^6(\bullet) = \nabla^2(\nabla^2(\nabla^2(\bullet)))$, $\nabla^4(\bullet) = \nabla^2(\nabla^2(\bullet))$, $\nabla^2(\bullet) = \frac{\partial^2(\bullet)}{\partial x^2} + \frac{\partial^2(\bullet)}{\partial y^2}$ is the Laplacian operator, $\acute{g} = 2G(1-v^2)/E_1h_1h_2$ is the shear parameter of the core, G is the shear modulus of the viscoelastic core, $Y = 3(1+h_2/h_1)^2$ is the geometric parameter, D_t is the total flexural rigidity, E_1 is Young's modulus of the face sheet, ν is the Poisson's ratio of the plate material, $M = \rho h$ is the mass per unit area of the entire sandwich, ρ is the total mass

density of the composite panel, h_1 and h_2, respectively, are the thicknesses of the face sheet and the constrained damping layer, $h = 2h_1 + h_2$ is the total thickness, and q is the external point force loading on the panel (Narayanan and Shanbhag (1982)). Figure 1 illustrates the geometrical configuration of the sandwich panel. If we consider the case of free vibration when $q(t, x, y) = 0$, and assume the plane wave $e^{i(\omega t - k_x x - k_y y)}$ propagating within the plate, we can reach the 6^{th} order dispersion relation via the six order problem defined by Eq.(1) as follows:

$$-D_t k^6 - D_t \acute{g}(1 + Y)k^4 + M\omega^2(k^2 + \acute{g}) = 0 \tag{2}$$

where $k = \sqrt{k_x^2 + k_y^2}$, and k_x and k_y are the wave numbers in the x and y directions, respectively.

2.2 4^{th} order problem

The shear effects are usually neglected for thin composite panels, and the flexural vibrating motions of such panels are usually expected to satisfy the 4^{th} order problem. According to the Kirchhoff-Love hypothesis and neglecting transverse shear and rotary inertia, the 4^{th} order problem governing the transverse displacement $w(x, y, t)$ of an undamped plate will be as follows (e.g. see Lesueur and Nicolas (1989); Jones (1999)):

$$D_{11}\frac{\partial^4 w}{\partial x^4} + 2(D_{12} + 2D_{66})\frac{\partial^4 w}{\partial x^2 \partial y^2} + D_{22}\frac{\partial^4 w}{\partial y^4} + M\frac{\partial^2 w}{\partial t^2} = q(t, x, y) \tag{3}$$

where $(x, y) \in [0, a] \times [0, b]$, D_{11}, D_{22}, D_{12}, and D_{66} are the bending rigidity coefficients, ρ is the mass density, h is the thickness, and $M = \rho h$ is the mass per unit area (herein, the geometrical configuration of the thin composite panel is the same as that of Figure 1, except for taking into account the core thickness).
The well-known particular case of the 4^{th} and 6^{th} order problems when $D_t = D_{11} = D_{22} = D_{12} + 2D_{66} = D$, and $g = 0$ presents the governing vibration motion of thin isotropic plates under Kirchhoff-Love hypothesis as follows (e.g. see Lesueur and Nicolas (1989); Jones (1999)):

$$D\nabla^4 w(x, y, t) + M\frac{\partial^2 w(x, y, t)}{\partial t^2} = q(t, x, y) \tag{4}$$

In the current study, this particular case has also been used for validating the efficiency of the proposed approach. In Section4, it has been used to model the

behavior of two isotropic panels for further validating the approach.
In the case of free vibration when $q(t,x,y)=0$, considering the wave $e^{i(\omega t-k_x x-k_y y)}$ propagating within the plate, the fourth order problem introduced by Eq.(3) leads to the 4^{th} order dispersion relation as follows:

$$D_{11}k_x^4+2(D_{12}+2D_{66})k_x^2k_y^2+D_{22}k_y^4-M\omega^2=0 \tag{5}$$

where k_x and k_y are the wave numbers in the x and y directions, respectively.

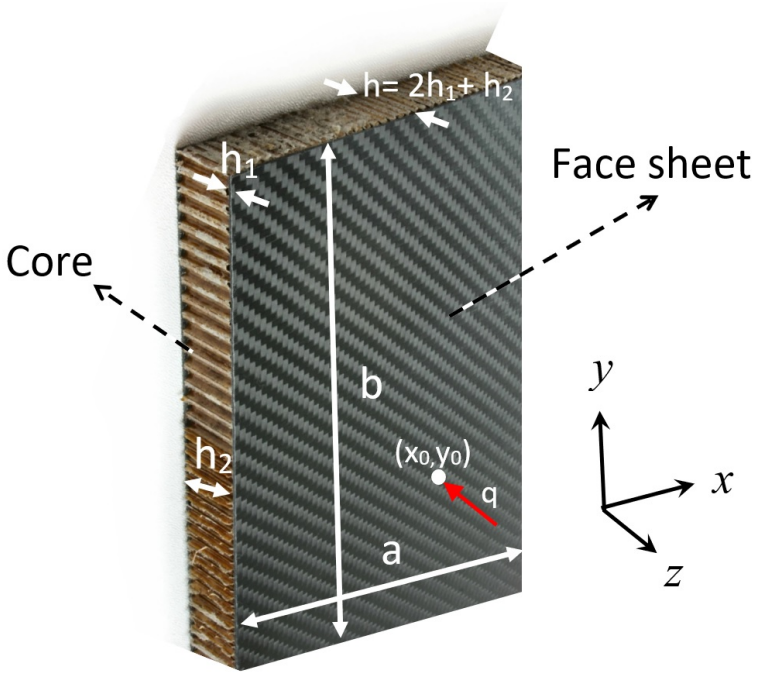

Figure 1: The geometrical configuration for a thick composite sandwich plate

2.3 Modal decomposition

By a modal decomposition and taking into account an ad hoc damping loss factor η for dissipation, the response H to a harmonic point force such $q(t)=e^{i\omega t}$ at point (x_0,y_0), will be as follows (e.g. see Lafont et al. (2014)):

$$H\left(x,y;x_0,y_0;\omega\right)=\sum_{n\geq 0}H_n\left(\omega\right)\psi_n\left(x_0,y_0\right)\psi_n\left(x,y\right) \tag{6}$$

where ψ_n denotes the modal function of mode n, the frequency response coefficient $\{H_n(\omega)\}$ is obtained as $H_n(\omega) = M^{-1}(\omega_n^2 - \omega^2 + i\eta\omega_n\omega)^{-1}$, and ω_n is the angular natural frequency belonging to the modal function ψ_n.
Based on the above modal decomposition for the harmonic response (i.e. Eq.6), the transverse displacement $w(x, y, t)$ can be modeled if the modes ψ_n can be correctly calculated. Thus, according to Eq.(6), the function $\tilde{w}(x, y; \omega)$ as the Fourier transform function of $w(x, y, t)$ is obtained by

$$\tilde{w}(x, y; \omega) = \sum_{n \geq 0} \tilde{q}(\omega) H_n(\omega) \psi_n(x_0, y_0) \psi_n(x, y) \tag{7}$$

where $\tilde{q}(\omega)$ is the Fourier transform of the external force $q(t)$. For instance, in a particular case when the boundary condition is simply supported, we can have an analytical expression for the modal functions as $\{\psi_n = (2/\sqrt{ab}) \sin(n_1\pi x/a) \sin(n_2\pi y/b)\}$ (e.g. see Lafont et al. (2014); Le Bot (2015)) but in reality, such expressions of modes are not enough and we should obtain reliable and accurate knowledge about them. In the next section, we will also see how the modal functions can be predicted in terms of hierarchical trigonometric functions, and then real laboratory measurements will assist us to have a reliable estimation of these critical functions.

3 Hybrid Updating Method

Herein, the methodology starts with the hierarchical functions required for modeling high-order bending modes and consequently modeling the flexural vibration. The variational formulation is analyzed via the hierarchical functions, and then the IWC technique is presented for performing an initial tuning to mechanical parameters used in the formulation. Afterward, the procedure of model updating is explained, and at last, the methodology ends with the least square optimization and updated values of the parameters. The structure and main stages of the proposed hybrid updating method are illustrated by Figure 2.

3.1 Hierarchical functions and formulations

Hierarchical functions are employed to model flexural motion of the plate structure where these functions are constructed by a type of trigonometric functions. The hierarchical functions can provide us with a better convergence rate when predicting high-order natural flexural modes of rectangular vibrating plates with any bound-

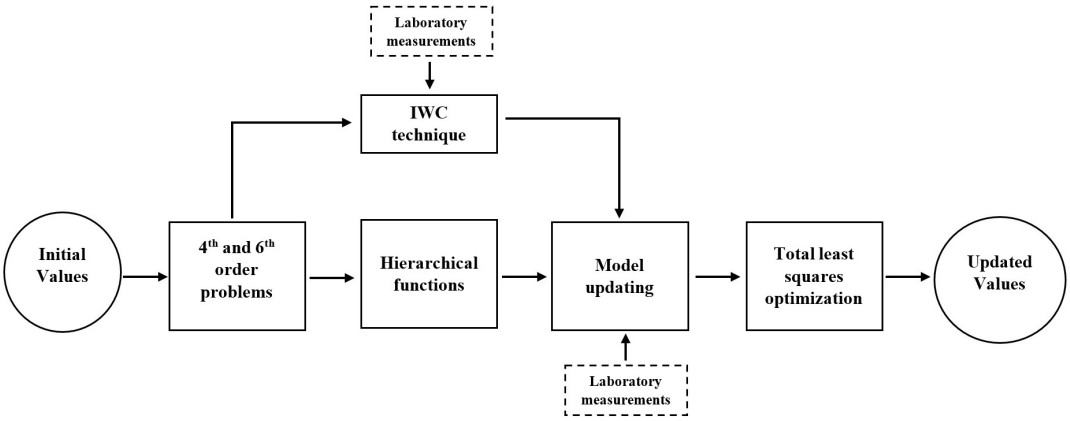

Figure 2: The schematic diagram illustrating the hybrid updating method

ary conditions (Beslin and Nicolas (1997)). Hence, according to the Rayleigh–Ritz method, the Fourier transform of the flexural displacement $\tilde{w}(x, y; \omega)$ can be approximated by the following relation (Beslin and Nicolas (1997); Jaouen et al. (2005)):

$$\tilde{w}(x, y; \omega) = \sum_{n} \tilde{w}_n(\omega)\phi_n(x, y) \tag{8}$$

where $\{\tilde{w}_n\}$ are complex coefficients, and the hierarchical functions $\{\phi_n\}$ are defined as follows:

$$\phi_n(x, y) = \alpha_l(\xi)\alpha_k(\eta) \tag{9}$$

where $n = n(l, k)$, and $\xi = 2x/a - 1$ and $\eta = 2y/b - 1$ are dimensionless space variables, and the functions $\{\alpha_l\}$ are of the following form (Beslin and Nicolas (1997); Jaouen et al. (2005)):

$$\alpha_l(\xi) = sin(a_l\xi + b_l)sin(c_l\xi + d_l) \tag{10}$$

where the coefficients $\{a_l, b_l, c_l, d_l\}$ are defined in Table 1, and meanwhile, the order l enables us to consider various Boundary Conditions (B.Cs) for the vibrating plate as follows:

- Free B.C: $l \geq 1$
- Simply Supported B.C: $l = 2, 4$ and $l \geq 5$
- Clamped B.C: $l \geq 5$

Table 1: The coefficients $\{a_l, b_l, c_l, d_l\}$ required for defining the hierarchical functions

	a_l	b_l	c_l	d_l
$l = 1$	$\pi/4$	$3\pi/4$	$\pi/4$	$3\pi/4$
$l = 2$	$\pi/4$	$3\pi/4$	$-\pi/2$	$-3\pi/2$
$l = 3$	$\pi/4$	$-3\pi/4$	$\pi/4$	$-3\pi/4$
$l = 4$	$\pi/4$	$-3\pi/4$	$\pi/2$	$-3\pi/2$
$l \geq 5$	$(l-4)\pi/2$	$(l-4)\pi/2$	$\pi/2$	$\pi/2$

Since the laboratory experiments were performed for vibrating plates under boundary conditions near the clamped boundary condition, from here on the clamped boundary condition is considered. However, according to the above-mentioned theories, the concepts of the methodology will remain the same for other types of conditions. Besides, in practice, the choice of a large value for parameter n in the Rayleigh–Ritz approximation (i.e. Eq.8) enables us to estimate a greater number of modes in the problem. On the other hand, to achieve convergence of the approximation and obtain an appropriate solution, the maximum number of modes should be appropriately selected for the modal decomposition (i.e. Eq.(7)). It is possible to demonstrate that the maximum number of modes N is a function of the desired maximum frequency when the problem is treated as a two-dimensional system (e.g. see chapter 6.3 in Le Bot (2015)). Now, according to the Rayleigh–Ritz approximation based on the hierarchical functions, we can reach variational formulations for both the 4^{th} and 6^{th} order problems.

3.1.1 For 4^{th} order problem

So, if the hierarchical function ϕ_m with the order m plays the role of a test function in the variational formulation for the 4^{th} order problem (see Eq.3), we will have the following equation for the case of free vibration (i.e. when $q = 0$):

$$\begin{aligned} D_{11}\int_0^b\int_0^a \frac{\partial^4\tilde{w}}{\partial x^4}\phi_m dxdy + 2(D_{12}+2D_{66})\int_0^b\int_0^a \frac{\partial^4\tilde{w}}{\partial x^2\partial y^2}\phi_m dxdy + \\ D_{22}\int_0^b\int_0^a \frac{\partial^4\tilde{w}}{\partial y^4}\phi_m dxdy - M\omega^2\int_0^b\int_0^a \tilde{w}\phi_m dxdy = 0 \end{aligned} \tag{11}$$

and subsequently, according to the Rayleigh–Ritz approximation (i.e. (8)), we will also have

$$D_{11}\sum_n \tilde{w}_n \int_0^b\int_0^a \frac{\partial^4\phi_n}{\partial x^4}\phi_m dxdy + 2(D_{12}+2D_{66})\sum_n \tilde{w}_n \int_0^b\int_0^a \frac{\partial^4\phi_n}{\partial x^2\partial y^2}\phi_m dxdy + D_{22}\sum_n \tilde{w}_n \int_0^b\int_0^a \frac{\partial^4\phi_n}{\partial y^4}\phi_m dxdy - M\omega^2\sum_n \tilde{w}_n \int_0^b\int_0^a \phi_n\phi_m dxdy = 0 \tag{12}$$

Thus, according to the integration by parts and the characteristics of the hierarchical functions defined for the clamped boundary condition (i.e. when $n, m \geq 5$), we have

$$D_{11}\sum_n \tilde{w}_n \int_0^b\int_0^a \frac{\partial^2\phi_n}{\partial x^2}\frac{\partial^2\phi_m}{\partial x^2} dxdy + 2(D_{12}+2D_{66})\sum_n \tilde{w}_n \int_0^b\int_0^a \frac{\partial^2\phi_n}{\partial x\partial y}\frac{\partial^2\phi_m}{\partial x\partial y} dxdy + D_{22}\sum_n \tilde{w}_n \int_0^b\int_0^a \frac{\partial^2\phi_n}{\partial y^2}\frac{\partial^2\phi_m}{\partial y^2} dxdy - M\omega^2\sum_n \tilde{w}_n \int_0^b\int_0^a \phi_n\phi_m dxdy = 0 \tag{13}$$

Accordingly, the above equation changes into $\mathbf{K}\tilde{\mathbf{w}} - \omega^2\mathbf{M}\tilde{\mathbf{w}} = \mathbf{0}$ where $\tilde{\mathbf{w}} = [\tilde{w_n}]$, and the stiffness matrix $\mathbf{K} = [K_{mn}]$ and mass matrix $\mathbf{M}$= $[M_{mn}]$ belonging to the 4^{th} order problem are defined as follows:

$$\mathbf{K} = [K_{mn}] = \left[\int_0^b\int_0^a (D_{11}\frac{\partial^2\phi_n}{\partial x^2}\frac{\partial^2\phi_m}{\partial x^2} + 2(D_{12}+2D_{66})\frac{\partial^2\phi_n}{\partial x\partial y}\frac{\partial^2\phi_m}{\partial x\partial y} + D_{22}\frac{\partial^2\phi_n}{\partial y^2}\frac{\partial^2\phi_m}{\partial y^2})dxdy\right] \tag{14}$$

$$\mathbf{M} = [M_{mn}] = \left[M\int_0^b\int_0^a \phi_n\phi_m dxdy\right] \tag{15}$$

3.1.2 For 6^{th} order problem

Similarly, based on the 6^{th} order problem introduced by Eq.1, we can also obtain the following formulation for the case of free vibration in the 6^{th} order problem (i.e. when $q = 0$):

$$D_t\int_0^b\int_0^a \nabla^6\tilde{w}\phi_m dxdy - D_t\acute{g}(1+Y)\int_0^b\int_0^a \nabla^4\tilde{w}\phi_m dxdy - M\omega^2\int_0^b\int_0^a (\nabla^2\tilde{w} - \acute{g}\tilde{w})\phi_m dxdy = 0 \tag{16}$$

So, subsequently, the Rayleigh–Ritz approximation (i.e. (8)) implies that

$$D_t \sum_n \tilde{w}_n \int_0^b \int_0^a \nabla^6 \phi_n \phi_m dxdy - D_t \acute{g}(1+Y) \sum_n \tilde{w}_n \int_0^b \int_0^a \nabla^4 \phi_n \phi_m dxdy \\ -M\omega^2 \sum_n \tilde{w}_n \int_0^b \int_0^a (\nabla^2 \phi_n - \acute{g}\phi_n)\phi_m dxdy = 0 \tag{17}$$

Therefore, using the integration by parts, and considering the characteristics of the hierarchical functions defined for the clamped boundary condition (i.e. the hierarchical functions with the orders $n, m \geq 5$), we will obtain

$$D_t \sum_n \tilde{w}_n \int_0^b \int_0^a \boldsymbol{\nabla}^3 \phi_n \cdot \boldsymbol{\nabla}^3 \phi_m dxdy + D_t \acute{g}(1+Y) \sum_n \tilde{w}_n \int_0^b \int_0^a \nabla^2 \phi_n \nabla^2 \phi_m dxdy \\ -M\omega^2 \sum_n \tilde{w}_n \int_0^b \int_0^a (\boldsymbol{\nabla}\phi_n \cdot \boldsymbol{\nabla}\phi_m + \acute{g}\phi_n \phi_m) dxdy = 0 \tag{18}$$

where the dot $\cdot$ is the sign of the inter product, $\boldsymbol{\nabla}^3(\bullet) = \boldsymbol{\nabla}(\nabla^2(\bullet))$, and $\boldsymbol{\nabla}(\bullet) = (\frac{\partial(\bullet)}{\partial x}, \frac{\partial(\bullet)}{\partial y})$ is the gradient operator. Consequently, the above relation is also formed into $\mathbf{K}\tilde{\mathbf{w}} - \omega^2 \mathbf{M}\tilde{\mathbf{w}} = \mathbf{0}$, and the stiffness matrix $\mathbf{K} = [K_{mn}]$ and mass matrix $\mathbf{M}$= $[M_{mn}]$ corresponding to the 6^{th} order problem are obtained as follows:

$$\mathbf{K} = [K_{mn}] = \left[\int_0^b \int_0^a D_t (\boldsymbol{\nabla}^3 \phi_n \cdot \boldsymbol{\nabla}^3 \phi_m + \acute{g}(1+Y) \nabla^2 \phi_n \nabla^2 \phi_m) dxdy \right] \tag{19}$$

$$\mathbf{M} = [M_{mn}] = \left[M \int_0^b \int_0^a (\boldsymbol{\nabla}\phi_n \cdot \boldsymbol{\nabla}\phi_m + \acute{g}\phi_n \phi_m) dxdy \right] \tag{20}$$

The above formulation for the 6^{th} order problem indicates that the stiffness and mass matrices are formed by (semi-) inner products of Sobolev spaces (cf. Adams and Fournier (2003)).

3.2 Inhomogeneous wave correlation technique

First, we need to have a certain initial knowledge about the mechanical parameters including Young modulus, Poisson ratio, shear modulus, and bending rigidity coefficients for constructing the governing equations. Although one can usually obtain such initial knowledge of the parameters from previous studies, and any

initial information about the parameters is enough to theoretically perform the updating procedure, and we do not expect much from their precision, in practice these initial values should be both reliable and acceptable. For this purpose, we can utilize methods of property identification for identifying effective structural properties. Hence, as introduced in Section 1, according to the abilities of the inhomogeneous wave correlation method (IWC) technique (Berthaut et al. (2005); Ichchou et al. (2008)), this approach can be helpful in this step, and hence, herein, we used IWC technique for initially tuning the mechanical parameters of composite panels before performing the model updating and associated optimizations. The IWC approach starts with an acquired full field of the vibrating panel, for constructing the k-space. This technique uses the acquired full field of vibration like w as the primary input, which can be acquired in a controlled laboratory condition via Laser precise Doppler Vibrometers (LDVs) or precise digital cameras. Then the correlation between the full field and an inhomogeneous wave $o_{k,\gamma.\theta}$ is calculated. This correlation leads us to a wavenumber-dependent objective function, the so-called Inhomogeneous Wave Correlation (IWC) as follows (Berthaut et al. (2005); Ichchou et al. (2008)):

$$\mathrm{IWC}(k,\gamma,\theta) = \frac{\left|\int_0^b \int_0^a w\overline{o}_{k,\gamma.\theta} dxdy\right|}{\sqrt{\int_0^b \int_0^a |w|^2 \, dxdy \int_0^b \int_0^a |\overline{o}_{k,\gamma.\theta}|^2 \, dxdy}} \tag{21}$$

where $o_{k,\gamma.\theta} = e^{-ik(\theta)(1+i\gamma(\theta))(x\cos(\theta)+y\sin(\theta))}$, $k(\theta)$ is the wave number in the direction θ, and $\gamma(\theta)$ is the wave attenuation defined by Lyon et al. (1995). So, the maximization of the above IWC objective function implies the identification of the complex wave number k for the given direction θ in the k-space. Then, based on the identified wave number in various directions of the k-space as well as considering the dispersion relations (i.e. (2) and Eqs.(5)), we can perform identification of mechanical properties of the composite panel too, see (Ichchou et al. (2008)). In the current study, this approach has been used for initially predicting the mechanical effective properties of panels before going through the model updating and associated optimization.

3.3 Model updating

Experimental knowledge about the full vibration field of the vibrating panel is required for adjusting the models and their associated parameters. Nowadays, such experimental data about the full vibration field can be acquired via advanced

scanning laser vibrometers or high-speed cameras (Stanbridge et al. (2004); Mottershead et al. (2011); Wang et al. (2011)). In this step, we apply the mode shapes, extracted from the full-field vibration data, acquired from laboratory experiments, to the models of the 4^{th} and 6^{th} order problems (in the next Section the procedure required for extracting the modes from the experimental data has been discussed). So, first assume that the columns of the matrix $\mathbf{\Psi}_M = [\psi_l^M] = [\psi_l^M(x_k, y_k)]$ contains the measured values of the mode shapes acquired in laboratory experiments (where ψ_l^M is the l^{th} column of the matrix $\mathbf{\Psi}_M$, which contains the measured values of the l^{th} modal function ψ_n, and $\psi_l^M(x_k, y_k)$ is the measured value of the l^{th} mode at the node k with coordinates (x_k, y_k)]). The measured values of the mode shapes should be projected to the hierarchical base functions. For this purpose, the measured values of the l^{th} mode shape at the node k can be approximated by the Rayleigh–Ritz method and hierarchical function as follows (see Eq.(8)):

$$\psi_l^M(x_k, y_k) = \sum_n \Psi_{nl}^M(\omega)\phi_n(x_k, y_k) \tag{22}$$

The above relation constitutes a system of linear equation, where on the left-hand side we have the measured values of the mode shapes $[\psi_l^M(x_k, y_k)]$, and on the right-hand side we have the known coefficients $[\phi_n(x_k, y_k)]$ (the known values of n^{th} hierarchical functions at the node k). So, by means of solving the above linear system, we can reach another form of the measured mode matrix $\mathbf{\Psi}_M = [\Psi_{nl}^M]$ that is actually the projection of the measured modes onto the hierarchical functions. Furthermore, before using this matrix it is recommended to normalize its columns in the following way: $\Psi_l := \Psi_l \left(\Psi_l^{\mathrm{T}} \mathbf{M} \Psi_l\right)^{-\frac{1}{2}}$ where Ψ_l is the l^{th} column of the matrix $\mathbf{\Psi}_M$ before normalization, i.e. Ψ_l is the measured l^{th} mode shape and formed by the hierarchical functions before normalization. For more information on this type of normalization (e.g. see Baruch (1978)).

Now, the measured values of the mode shapes are ready to be used by the model updating. Thus, for the 4^{th} and 6^{th} order problems (see Subsections 3.1.1 and 3.1.2) if we suppose that the stiffness matrix $\mathbf{K}$ is more affected by the uncertainties than the mass matrix $\mathbf{M}$, we can consider the mass matrix $\mathbf{M}$ as the reference matrix. So, by means of the following least squares optimization, Baruch method, we can find the correction to the stiffness matrix $\delta\mathbf{K}$ as well as the optimized matrix of mode shapes $\hat{\mathbf{\Psi}}$ as follows (see Baruch (1978); Humbert (1999)):

$$\begin{cases} \left\|\mathbf{M}^{-\frac{1}{2}}\delta\mathbf{K}\mathbf{M}^{-\frac{1}{2}}\right\|_F^2 \rightarrow Min \\ \hat{\mathbf{K}}\hat{\mathbf{\Psi}} = \mathbf{M}\hat{\mathbf{\Psi}}\mathbf{\Omega}_M^2 \\ \hat{\mathbf{K}} = \hat{\mathbf{K}}^{\mathrm{T}} \end{cases}, \quad \begin{cases} \left\|\mathbf{M}^{\frac{1}{2}}\delta\mathbf{\Psi}\right\|_F^2 \rightarrow Min \\ \hat{\mathbf{\Psi}}^{\mathrm{T}}\mathbf{M}\hat{\mathbf{\Psi}} = \mathbf{I} \end{cases} \tag{23}$$

where $\delta\mathbf{K} = \hat{\mathbf{K}} - \mathbf{K}$, and $\delta\mathbf{\Psi} = \hat{\mathbf{\Psi}} - \mathbf{\Psi}_M$ is the correction to the mode shapes, also, $\|\bullet\|_F$ is the Frobenius norm, and Ω_M is a diagonal matrix whose diagonal elements consists of measured values of angular natural frequencies corresponding to the measured modes. Baruch (1978) showed that the solution to the above optimization will be as follows:

$$\begin{gathered} \delta\mathbf{K} = -\mathbf{K}\hat{\mathbf{\Psi}}\hat{\mathbf{\Psi}}^{\mathrm{T}}\mathbf{M} - \mathbf{M}\hat{\mathbf{\Psi}}\hat{\mathbf{\Psi}}^{\mathrm{T}}\mathbf{K} + \mathbf{M}\hat{\mathbf{\Psi}}\hat{\mathbf{\Psi}}^{\mathrm{T}}\mathbf{K}\hat{\mathbf{\Psi}}\hat{\mathbf{\Psi}}^{\mathrm{T}}\mathbf{M} + \mathbf{M}\hat{\mathbf{\Psi}}\Omega_M^2\hat{\mathbf{\Psi}}^{\mathrm{T}}\mathbf{M} \\ \hat{\mathbf{\Psi}} = \mathbf{\Psi}_M(\mathbf{\Psi}_M^{\mathrm{T}}\mathbf{M}\mathbf{\Psi}_M)^{-\frac{1}{2}} \end{gathered} \tag{24}$$

Herein, the above solution enables us to update the associated stiffness matrices obtained by Eqs.(14) and (19), and consequently, it will enable us to update the corresponding parameters of the 4^{th} and 6^{th} order problems as discussed in the following subsection.

3.4 Total least squares optimization

Accordingly, suppose that the vector $\mathbf{p} = [p_i]$ consists of the parameters to be updated. We know that the stiffness matrix is a function of the parameters (i.e. $\mathbf{K} = \mathbf{K}(\mathbf{p})$ and $K_{nm} = K_{nm}([p_i])$). Hence, we have

$$\delta K_{nm} = \sum_i \frac{\partial K_{nm}}{\partial p_i}\delta p_i \tag{25}$$

So, considering the correction to the stiffness matrix $\delta\mathbf{K} = [\delta K_{nm}]$ obtained via Eq.(24) and laboratory experiments, the above equation for all the elements of the matrix $\delta\mathbf{K} = [\delta K_{nm}]$ constitutes a system of linear equations like $\mathbf{b} = \mathbf{A}\mathbf{x}$ where $\mathbf{x}$ as the unknown vector consists of the corrections to the parameters ($\mathbf{x} = \delta\mathbf{p} = [p_i]$), the vector $\mathbf{b} = [\delta K_{nm}]$ as the known data consists of the elements of $\delta\mathbf{K}$ obtained via Eq.(24), and the matrix $\mathbf{A} = [\frac{\partial K_{nm}}{\partial p_i}]$ is formed by the derivatives of the elements of the stiffness matrix as discussed in the following.

3.4.1 For 4^{th} order problem

For the 4^{th} order problem, we have three independent parameters, which can be estimated via the above-mentioned linear problem. According to (14) formulating the stiffness matrix of the 4^{th} order problem via the hierarchical functions, the three independent parameters are $p_1 = D_{11}$, $p_2 = D_{12} + 2D_{66}$, and $p_3 = D_{22}$, and we have (see (14))

$$\frac{\partial K_{mn}}{\partial p_1} = \frac{\partial K_{mn}}{\partial D_{11}} = \int_0^b \int_0^a \frac{\partial^2 \phi_n}{\partial x^2} \frac{\partial^2 \phi_m}{\partial x^2} dxdy \tag{26}$$

$$\frac{\partial K_{mn}}{\partial p_2} = 2 \int_0^b \int_0^a \frac{\partial^2 \phi_n}{\partial x \partial y} \frac{\partial^2 \phi_m}{\partial x \partial y} dxdy \tag{27}$$

$$\frac{\partial K_{mn}}{\partial p_2} = \frac{\partial K_{mn}}{\partial D_{22}} = \int_0^b \int_0^a \frac{\partial^2 \phi_n}{\partial y^2} \frac{\partial^2 \phi_m}{\partial y^2} dxdy \tag{28}$$

3.4.2 For 6^{th} order problem

Also, for the 6^{th} order problem, we have two independent parameters whose corrections can also be estimated by Eq.(25). Hence, according to (19) formulating the stiffness matrix of the 6^{th} order problem via the hierarchical functions, the two independent parameters are the total flexural rigidity $p_1 = D_t$, and the shear parameter of the core $p_2 = g'$, and we have (see (19))

$$\frac{\partial K_{mn}}{\partial p_1} = \frac{\partial K_{mn}}{\partial D_t} = \int_0^b \int_0^a \boldsymbol{\nabla}^3 \phi_n \cdot \boldsymbol{\nabla}^3 \phi_m dxdy \tag{29}$$

$$\frac{\partial K_{mn}}{\partial p_2} = \frac{\partial K_{mn}}{\partial g'} = (1+Y) \int_0^b \int_0^a \nabla^2 \phi_n \nabla^2 \phi_m dxdy \tag{30}$$

3.4.3 Updating parameters

Accordingly, now we can solve Eq.(25) for finding the corrections to the parameters and consequently updating the parameters. Herein, we employed the total least squares method (TLS) for adjusting and solving Eq.(25). The total least squares method is a natural generalization of the least squares method, recommended for solving a system of linear equations when all the given data including both the

model $\mathbf{A}$ and $\mathbf{b}$ suffer from uncertainties, and it has a wide range of applications in system theory, signal processing, and computer algebra (Markovsky and Van Huffel (2007)). In order to estimate the residual parameters $[\delta p_i]$ and subsequently update the parameters $[p_i]$, according to the total least squares method, the solution to the equation Eq.(25) formed into $\mathbf{b} = \mathbf{A}\mathbf{x}$ will be as follows (see Markovsky and Van Huffel (2007)):

$$\delta\hat{\mathbf{p}} = \hat{\mathbf{x}} = (\mathbf{A}^{\mathrm{T}}\mathbf{A} - \sigma_{n+1}^2\mathbf{I})^{-1}\mathbf{A}^{\mathrm{T}}\mathbf{b} \tag{31}$$

where the elements of $\mathbf{A} = [\frac{\partial K_{nm}}{\partial p_i}]$ are obtained by Eqs.(26) to (29), σ_{n+1} is the smallest singular value of the matrix $[\mathbf{A}\ \mathbf{b}]$, and $\mathbf{I}$ is the identity matrix. So, at last the updated parameters $\hat{\mathbf{p}}$ will be obtained by adding the estimated corrections $\delta\hat{\mathbf{p}}$ to the initial parameters $\mathbf{p}$ (i.e. $\hat{\mathbf{p}} = \mathbf{p} + \delta\hat{\mathbf{p}}$).

4 Experiments

We chose four plates including a thick sandwich composite plate (with a Nomex honeycomb core), and a Carbon-Fiber-Reinforced Polymer (CFRP) laminate composite plate as well as two isotropic plates (aluminium and steel ones). Nomex honeycomb cores have been widely used in composite sandwich panels. Nomex (DuPont de Nemours, Inc.) honeycomb cores can be an appropriate choice for manufacturing thick sandwich panels concerning their environmental resistance, flammability properties, dielectric properties, and galvanic compatibility with face sheets (Roy et al. (2014)). On the other hand, Carbon fiber reinforced plastics (CFRP) laminate is a type of composite panel, which is made of extremely strong and light fiber-reinforced plastics that contain carbon fibers, have found extensive usage as structural components in various types of advanced structures (cf. Qi et al. (2019)). In addition to the two composite plates, we also examined two isotropic ones (aluminium and steel). The usage of the isotropic plates had the advantage that the updating approach could additionally be tested and validated for the special case of the 4^{th} order equation (i.e. Eq.(4)) that is applicable for isotropic plates, too.

In this study, the above experimental plates sometimes referred to as specimens, are examined in controlled laboratory conditions in a semi-anechoic chamber whose dimensions were $3.4m(W) \times 5m(L) \times 1.9m(H)$. The semi-anechoic chamber possessed a measuring window (with dimensions $60cm \times 40cm$), which could be used for vibroacoustic measurements of vibrating plates (the semi-anechoic room was coupled to another untreated room) (see Figure 4).

4.1 Experimental set-up

The experimental set-up of the current study has been summed up by Figure 3, and some views of the laboratory configuration have been shown by Figure 4. For performing vibration measurements, a scanning laser vibrometer system (PSV-300-F/S High Frequency Scanning Vibrometer System), manufactured by Polytec Co., has been used. The scanning laser vibrometer system was used to measure the full-vibration field associated with the flexural displacement of the vibrating plates from the inside of the semi-anechoic chamber when the plates were been shaken from the other side of the measuring window (see Figure 4). The specimens were installed in the $40cm \times 60cm$ measuring window in such a way that the boundary condition of the vibrating plates was similar to a clamped boundary condition. For this purpose, in the experiments of each specimen, all the screws of the measuring window frame were installed with a torque of 30Nm (see Figure 4 (b)). Also, a shaker was used for a point-wise excitation of the plates from the back while it was attached to a piezoelectric sensor as the force transducer with sensitivity 105.5mV/N for measuring and sending the force signal to the spectrum analyzer (see Figure 4 (c)). In addition to the laser measurements, the sound radiated from the vibrating plates in the semi-anechoic chamber was recorded at a distance of 50cm from the middle of the vibrating plates. Herein, the sounds were recorded with an omnidirectional microphone, manufactured by Brüel & Kjær Co., with a sensitivity equal to 27.3mV/Pa. After calibration, the sound pressure level (SPL) was calculated. Figure 4 (e) illustrates the microphone facing the vibrating plate and recording the sounds. Also, the scanning laser system was equipped with a spectrum analyzer acquiring the signals sent from the laser vibrometer as well as other sensors including the piezoelectric sensor and the microphone. The spectrum analyzer enabled a white noise signal to be generated and sent to a signal generator for producing the voltage required by the shaker. Then, the laser vibrometer, microphone, and piezoelectric sensor of the force transducer simultaneously sent their signal to the spectrum analyzer that gathered the spectra of all the data in a unique database including the spectra belonging to all the sensors.

4.2 Characteristics of specimens

The four specimens had the dimensions $42cm \times 62cm$ that could be clamped and installed in the measuring window. One of the specimens was a thick sandwich plate with a Nomex honeycomb core covered by two face sheets, and its total

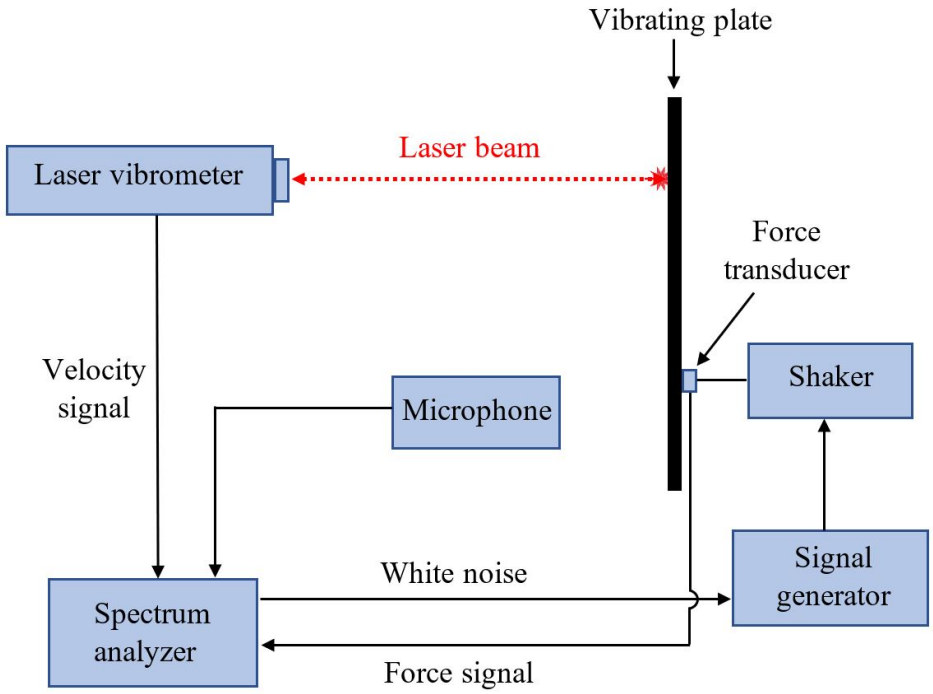

Figure 3: The schematic diagram of the experimental set-up

thickness was equal to 13.9mm. The two face sheets of this composite structure are made of two CFRP plates, seemingly woven, surrounding the Nomex honeycomb core, where the thickness of each face sheet and core is 0.2mm and 13.5mm, respectively. According to the literature, we could have an initial prediction on some characteristics of the core. According to the mechanical characterization study of Nomex honeycomb core done by Zhou et al. (2021), the equivalent shear modulus of the core was initially taken as 50Mpa. Also, each face sheet was initially assumed to be equivalent to a laminate composed of CFRP plys with a layout [0/90]. According to the studies of Shahdin et al. (2011); Qi et al. (2019); Zhou et al. (2021), the mechanical properties of the CFRP plys with epoxy matrix after curing were considered as what presented in Table 2. The other specimen was a composite laminate plate made of 25 CFRP plys with a symmetric layout as [(+45/-45/0/+90/0/+45/-45/0/+90/0/+45/-45)2 0]S. For this laminate plate, herein sometimes called a thin composite plate, the mechanical characteristics of each ply after curing were also assumed to be equal to what is presented in Table 2. The aforementioned values of the mechanical properties for each component of the two composite panels enabled the study to have an initial evaluation of the

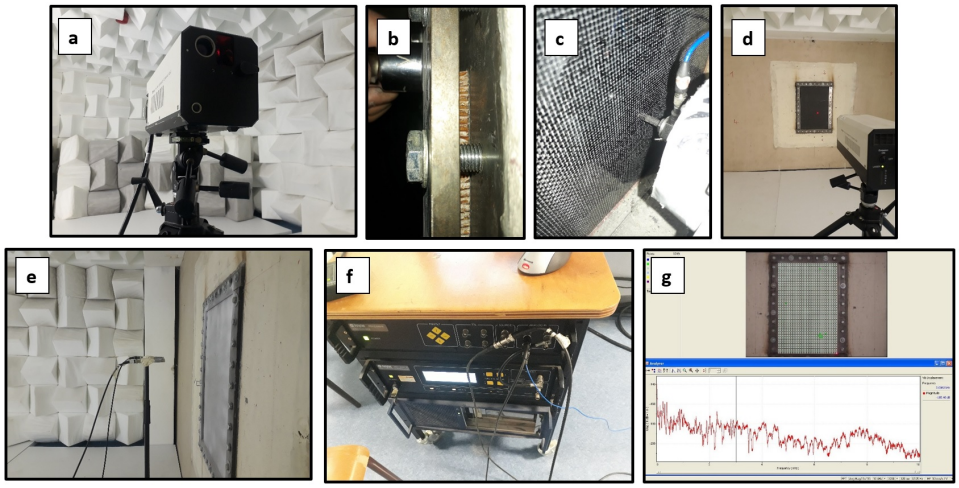

Figure 4: Some views of the configuration associated with the laboratory experiments: a) the PSV-300-F/S Scanning Vibrometer head, b) the clamped boundary condition performed with a torque equal to 30Nm for screws of the window frame, c) the shaker attached to the plate and connected to a piezoelectric sensor sending the force signal, d) the measuring window, and the floor covered by soundproofing forms e) the microphone recording the sound, f) the spectrum analyzer, g) the spectrum analyzer software

effective mechanical properties of the composite panels. Accordingly, a prediction on the equivalent values of the bending stiffness coefficients could be obtained by calculating the ABD stiffness matrix in classical laminate theory (CLT) where the bending stiffness could be initially estimated as follows:

$$D_{ij} = \frac{1}{3}\sum_{k} \bar{Q}^{k}_{ij}(z^{3}_{k} - z^{3}_{k-1}) \tag{32}$$

where $[\bar{Q}^{k}_{ij}]$ is the transformed reduced stiffness matrix, z_k is the represents the vertical position in the k^{th} layer of the composite plate from the mid-plane measured in meters, and $i, j = 1, 2, 6$ (e.g. see Kaw (2005); Daniel et al. (2006)). In addition, we had a 3mm thick aluminum plate, as well as a 0.85mm thick steel plate. At the initial step, the Young modulus and Poisson ratio of the aluminium specimen were presumed to be equal to 70GPa and 0.33, and also, for the steel specimen to be equal to 210GPa and 0.28, respectively. Furthermore, the precise values of the mass density associated with specimens could be obtained via measuring the dimensions and the weights of the specimens. Thus, the measured values of the mass densities corresponding to the composite thick sandwich, thin composite laminate, and the aluminium and steel plates have been obtained equal

Table 2: The initial information on the mechanical parameters. The mechanical properties of each CFRP ply with epoxy matrix after curing are based on the assessments of Shahdin et al. (2011); Qi et al. (2019); Zhou et al. (2021), and those of the Nomex core are based on the studies of Adams and Maheri (1993); Zhou et al. (2021). The mass densities were measured in the laboratory experiments

	E_1	E_2	G_{12}	ν	h [mm]	ρ [kg/m^3]
CFRP ply	140 GPa	7 GPa	3 GPa	0.3	0.14-0.2	1506
Nomex core	100 MPa	100 MPa	50 MPa	0.25	13	80
Aluminium	70 GPa	70 GPa	30 GPa	0.33	3	2648
Steel	210 GPa	210 GPa	80 GPa	0.29	0.85	7769

to 138, 1506, 2648, and 7769 kg/m^3, respectively.
Accordingly, we could reach initial approximations of the flexural bending stiffness coefficients associated with the plates. According to Table 2, the shear modulus of the composite sandwich was assumed to be equal to 50MPa, and its total flexural stiffness coefficient D_t required by the 6^{th} order problem (see Eq.(1)) was obtained equal to 935Nm. Similarly, according to the initial information on the mechanical parameters, the flexural bending stiffness corresponding to the aluminium and steel plates were equal to 176Nm, and 12Nm, respectively. Besides, according to Eq.(32) as well as the information of Table 2, the orthotropic bending coefficients of the thin composite laminate plate were equal to $D_{11} = 237$Nm, $D_{22} = 163$Nm, $D_{12} = 72$Nm, and $D_{66} = 75$Nm. In this work, at the initial stage, we used these initial values of the bending stiffness for providing an initial prediction on the vibroacoustic behaviors of the specimens when they are mechanically excited with a white-noise point-wise force.

4.3 Vibration measurements

The full-field vibration measurements for all the specimens were performed via the PSV-300-F/S laser doppler vibrometer (LDV) while the shaker was exerting a point-wise excitation with a white-noise behavior to the specimens. The analyzer of the PSV-300-F/S system provided the shaker with the white noise signal, and the LDV enabled non-contact vibration measurements of the specimens' surfaces to be undertaken. The LDV directed laser beams at the surface of interest,

and the vibration amplitude and frequency were extracted from the Doppler shift of the reflected laser beam frequency due to the motion of the vibrating plates. Originally, the output of an LDV is a continuous signal presenting the velocity field of the vibrating plates, which could be converted to the full-filed vibration field. Also, herein, we performed the laser scanning on 1855 nodes for both the sandwich and laminates plates, and on 2109 and 2035 nodes for the aluminum and steel plates, respectively. It means that the average spatial resolution of the laser scanning was between 0.87cm to 0.94cm. The measurement acquired for the frequency range [3.125Hz, 10kHz] with the frequency resolution equal to 3.125Hz. Since one of the future goals of this research is the use of the measurements in future psychoacoustic experiments, herein the maximum frequency range of the LDV system (i.e. [3.125Hz, 10kHz]) has been selected to perform measurements. For extracting the natural frequencies and their corresponding mode shapes from the full-field vibration field, we adopted a technique for the identification of frequency response function (FRF), based on the concept of the Single-input multiple-output (SIMO) systems. For this purpose, first, a number of the laser observation nodes for each plate were selected, where the velocity was measured for the desired frequency range [3.125Hz, 10kHz]. Then considering the observed force signal as a single-input (SI) and considering the measured velocity as the Multiple-outputs, we could form a SIMO system, and hence, its natural frequencies could be extracted from the system by the Least-Squares Complex Exponential Method. The least-squares complex exponential method estimates the FRF corresponding to each Single-input multiple-output (SIMO) system and fits to the response a set of complex damped sinusoids using Prony's method (see Heylen et al. (1997);He and Fu (2001);Brandt (2011); Ozdemir and Gumussoy (2017)). In the next step, the measured values of the model shapes were used in the updating procedures.

4.4 Updating procedures

First, parameter identification was performed for the problems formulated by the hierarchical functions. Although prior knowledge of the properties of the specimens' components (cf. Table 2 and Section 4.2) can be helpful to have a prediction on the mechanical parameters of the specimens, in practice such prior information may be far from the reality and may mislead the problems about the true solutions. As described in Section 3.2, the identification of the properties was performed by the IWC technique. For this purpose, considering the full-field vibration measurements for each specimen, the wave numbers corresponding to 20 frequencies

Table 3: The mechanical properties of the composite sandwich, laminate, aluminium, and steel plates, identified by the IWC technique

Sandwich	Laminate	Aluminium	Steel
$D_t = 1093\text{Nm}$	$D_{11} = 259\text{Nm}$, $D_{22} = 136\text{Nm}$	$E = 76\text{GPa}$	$E = 213\text{GPa}$
$G_c = 68\text{MPa}$	$D_{12} + 2D_{66} = 189\text{Nm}$		

and in 180 directions could be extracted from the measurements by means of the maximization of the IWC function (see Eq.(21)). Herein, for the frequencies, the center frequencies of one-third octave bands from 125Hz to 10kHz were used, and the 180 directions were equal to 1 degree to 180 degrees. On the other hand, the dispersion equations enable mathematical relationships between the frequencies, their corresponding wave numbers, and the mechanical properties (see Eqs.(5) and (2)). So, these mathematical relationships could provide us with a system of equations finding the mechanical properties of the specimens (see Ichchou et al. (2008)). Table 3 summarizes the properties obtained by the IWC technique.

In the next step, the mechanical parameters identified by the IWC technique were used in the model updating procedures. Herein, the 6^{th} order problem (i.e. Eq.(1)) was used for the formulation and modeling associated with the thick composite sandwich plate; the 4^{th} order problem with its general form (i.e. Eq.(3)) was used for the modeling of the thin composite laminate specimen, and also, the particular case of the 4^{th} order problem adapted for thin isotropic plates (i.e. Eq.(4)) was also utilized for the formulation and modeling corresponding to the aluminium and steel plates. Therefore, applying the identified parameters to the analytical formulations of the stiffness and mass matrices introduced by the hierarchical functions (i.e. Equations (14), (15), (19), and (20)), we could analytically calculate these matrices, and then apply them to the model updating solution (i.e. Eq. (24)). The model updating solution requires the measured mode shapes, which we could extract from the full-field laser measurement. The updated modal shapes are one of the main outputs of the model-updating procedures (see (24)), and since they are essentially needed for the modal decomposition and for finding the final solution to the problem, we need to have an idea on their quality. Modal Assurance Criterion (MAC) is a type of correlation criterion, which makes it possible to measure the quality of calculated mode shapes, and also enables to match two families of modes. For instance, for the calculated and measured modes, the

cross MAC is defined and calculated as follows (e.g. see Humbert (1999)):

$$MAC(\psi_l^M, \psi_l) = \frac{\left|\psi_l^M \cdot \psi_l\right|}{\sqrt{\psi_l^M \cdot \psi_l^M}\sqrt{\psi_l \cdot \psi_l}} \tag{33}$$

where $\cdot$ denotes the inner product, and the vectors ψ_l^M and ψ_l are the l^{th} measured and calculated modes, respectively. The MAC values are between 0 and 1, and a value close to 1 indicates a good correlation between the calculated and measured modal shapes. In Figures 5 to 8, the MAC values have been illustrated for cases performed before and after the updating procedures. As seen in these figures, after applying the updating procedures to the modal shapes, we can see that the values of the cross MAC have been enhanced for all the calculated modes associated with all the plates. The figures demonstrate that the updating procedures for the problems associated with the 4 specimens could enhance the MAC matrices by decreasing the elements other than the diagonal and increasing the diagonal elements of the MAC matrices and pushing them toward 1 (for example, compare Figures 5 (a) and (b)). It means that the updated mode shapes are closer to the real measured values by comparison with the old ones obtained before the updating while they also satisfy the 4^{th} or 6^{th} order problems. In fact, at the first step, the hierarchical functions could provide reliable modelings of the problems, and they were so helpful in presenting the approach with the required formulations, but in practice, such modelings are not enough for precise vibroacoustic predictions, and the updating procedures based on real data are required, which can enhance the modeling and its corresponding parameters, and move the models towards the reality. Herein, the MAC shows such achievement in bringing modeling to reality. Consequently, based on Eq.(31)), the updating approach will present the required corrections to the parameters identified by the IWC approach, and find the final updated parameters for each specimen. Table 4 has summarized the corrected values of the mechanical parameters.

In the above-mentioned procedures for identifying the parameters, we did not use the initial information (Table 2) on the mechanical parameters. As mentioned before, we used this initial knowledge only for obtaining a prediction of the vibroacoustic behaviors of the specimens, and now these values can be helpful to have an independent assessment of the updated parameters. The presented approach only depends on the IWC approach for identifying the parameters before the model updating procedures. Comparing Table 4 and Table 2, we can realize that although the updated values and the initial values have been obtained inde-

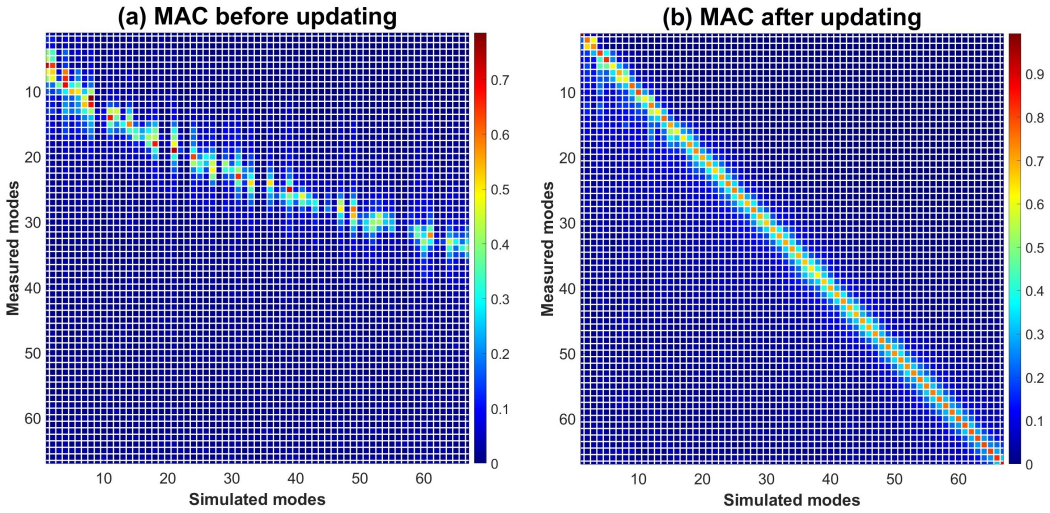

Figure 5: The MAC corresponding to the composite sandwich specimen: a) a view of the elements of the MAC matrix before the updating, and b) after the updating

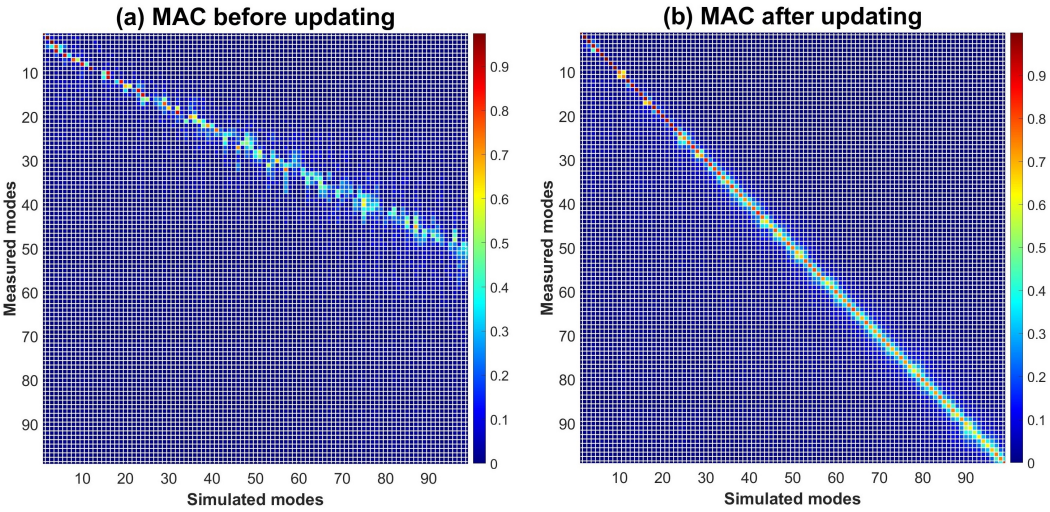

Figure 6: The MAC corresponding to the composite laminate specimen: a) a view of the elements of the MAC matrix before the updating, and b) after the updating

pendently, they are close to each other. For instance, the estimated total bending stiffness of the composite sandwich plate $D_t = 1034$Nm (see table 4) implies that the Young modulus of the face sheet to be equal to 153GPa. This value is in good agreement with the assessments of Qi et al. (2019) if the mechanical properties of the face sheet are approximated by a CFRP laminate with layout [0/90]. Qi et al.

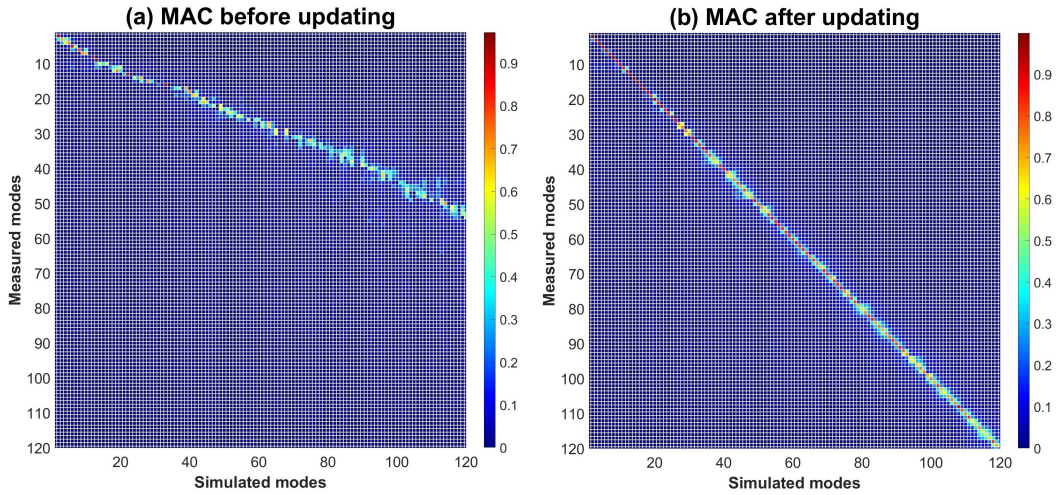

Figure 7: The MAC corresponding to the aluminium specimen: a) a view of the elements of the MAC matrix before the updating, and b) after the updating

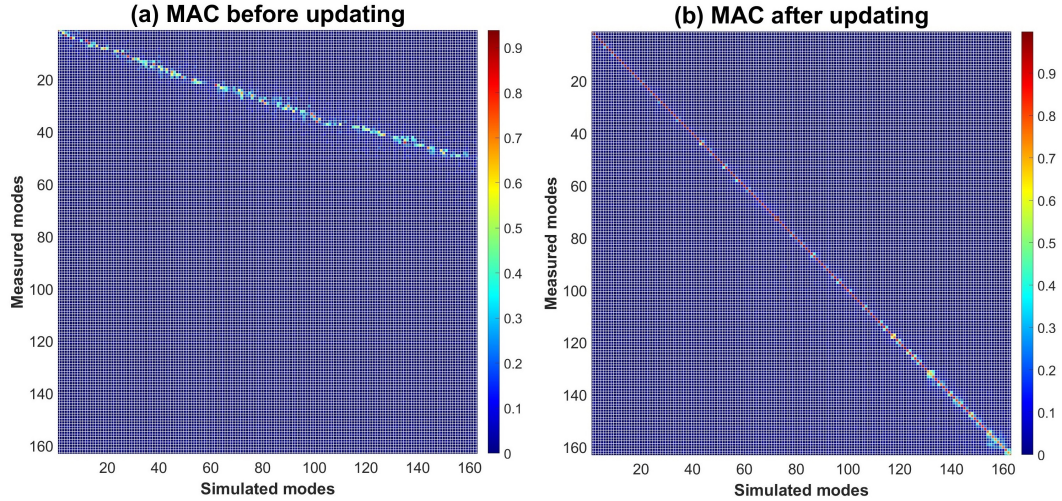

Figure 8: The MAC corresponding to the steel specimen: a) a view of the elements of the MAC matrix before the updating, and b) after the updating

(2019) proposed a method for predicting the mechanical properties of CFRP based on cross-scale simulation. In this study, a series of experiments were performed in order to show that the results of the prediction approach and the experiments are in good agreement. The preliminary information on mechanical properties of the CFRP ply, summarized in Table 2, is based on this research. Moreover, considering this research, the values of the mechanical properties of the CFRP could

Table 4: The updated mechanical properties of the composite sandwich, laminate, aluminium, and steel plates

Sandwich	Laminate	Aluminium	Steel
$D_t = 1034$Nm	$D_{11} = 274$Nm, $D_{22} = 126$Nm	$E = 74$GPa	$E = 202$GPa
$G_c = 71$MPa	$D_{12} + 2D_{66} = 182$Nm		

present a prediction on the flexural bending stiffness coefficients of the laminate plate, too. For this purpose, considering the layout [(+45/-45/0/+90/0/+45/-45/0/+90/0/+45/-45)2 0]S for the composite laminate plate, and based on Eq. (32) and Table 2, the flexural bending stiffness coefficients of the laminate were obtained as $D_{11} = 237$Nm, $D_{22} = 163$Nm, $D_{12} = 72$Nm, and $D_{66} = 75$Nm, which are in a good agreement with both the IWC results (cf. Table 3), and the updated parameters (Table 4). Furthermore, the Nomex core shear modulus, which is identified by the IWC approach and updated by the updating approach, is not far from the assessments of the studies carried out by Adams and Maheri (1993) and Zhou et al. (2021). Table 2 includes an approximate prediction on the mechanical properties of Nomex honeycomb, based on the studies of Adams and Maheri (1993), and Zhou et al. (2021).

4.5 Vibroacoustic comparisons

For the vibroacoustic assessment of the proposed approach, we made two types of comparisons using vibration measurements (acquired by the LDV instrument), and SPL recorded by the microphone. Figure 9 illustrates a comparison between the average of the measured vibration field and the simulated one for the frequency interval [0Hz,3kHz]. In this figure, it is clearly seen that the updating procedures could significantly enhance the simulations performed based on the sixth-order problem. In this figure, the agreement of the average value of the simulated vibration after updating with the actual value taken with the laser system is clearly evident. On the other hand, the disparity between the simulated values prior to the updating and the measured values may primarily be attributed to uncertainties in the initial values of mechanical parameters and the unknown intricacy of the boundary conditions, necessitating the usage of the updating method.
Moreover, according to these results, it is understood that the Root Mean Square (RMS) of the errors associated with the simulations in the two states after and

before the updating for the composite panel was 4.32×10^{-7}m and 2.44×10^{-8}m, respectively, and this means that the updating method has the ability to improve the simulation by around 17.7 times from this point of view (herein, the simulation error is obtained from the difference between the simulation values and the values taken with the LDV system).

In addition, the same comparison between the sound pressure levels of the sounds radiated from the vibrating plate has been carried out. The SPL at a distance of 50cm from the middle point of the vibrating plates, has also been acquired for the additional assessment of the updating approach. The measured sound pressure spectrum was compared with the simulated ones. For simulating the SPL at an arbitrary distance from the vibrating plate in the semi-anechoic chamber, we used the modeled full-vibration field and the well-known Rayleigh integration with time dependence $e^{i\omega t}$ as follows (e.g. see Fahy (2000)):

$$p\left(x,y,z;\omega\right) = i\omega\rho_0 \iint_S v(x',y')\frac{e^{ikR}}{2\pi R}dx'dy' \tag{34}$$

where the plate is supposed to be embedded in a rigid baffle, the acoustic pressure is assumed to be radiated from the plate in fluid half-space $z > 0$, $p\left(x,y,z;\omega\right)$ is the pressure field at the location (x,y,z), ω is the angular frequency, ρ_0 is the air density, $v\left(x',y'\right)$ is the vibration velocity at the point (x',y')located in the plate area S, $k = \frac{\omega}{c_0}$ is the wavenumber, c_0 is the sound speed in the air, and $R = \sqrt{(x-x')^2 + (y-y')^2 + z^2}$. The modal decomposition described in Section 2.3 is employed for modeling the velocity $v = \omega w$, and the displacement field w over the plate. For this purpose, the updated modes were used, and the frequency response could be obtained by the natural frequencies estimated by the Least-Squares Complex Exponential Method, introduced in Section 4.3. Besides, this method had the ability to present us with an average prediction on the loss damping factor η of the specimens. The least-squares complex exponential method can be utilized to analyze the frequency response function (FRF) of vibration obtained from the laser measurements. In fact, the least-squares complex exponential method applies the Prony's method to the FRF, which allows to fit a collection of complex damped exponential functions to the FRF, using a least squares optimization. The complex exponential functions represent the modes present in the FRF, and meanwhile, the poles of these complex damped exponential functions correspond to the complex frequencies at which the FRF exhibited decay and oscillation. By estimating the damping ratios using the complex frequencies, namely the poles, the loss damping factors can be determined too (see chapter 9.5 in He

and Fu (2001)). Accordingly, the average loss damping factor for the composite sandwich, laminate, aluminium, and steel plates were equal to 0.0916, 0.0451, 0.0158, and 0.0087, respectively. The range of these average values is consistent with prior research that has explored nearly related case studies regarding the loss damping factor (e.g. see Ghinet and Atalla (2011); Li and Narita (2013); Cherif et al. (2015); Sarlin et al. (2012)).

In addition, the measurements allowed for the calculation of modal density and modal overlap factor (MOF). Modal density was determined by counting the natural frequencies that were detected by the Least-Squares Complex Exponential Method. The MOF could also be calculated by incorporating the loss damping factor (η) and the modal density (d) for a given frequency (f), resulting in the equation MOF $= d\eta f$. The findings revealed that the average modal densities for the composite sandwich, laminate, aluminium, and steel plates were 0.007, 0.01, 0.012, and 0.016, respectively. Correspondingly, the average MOF values were 3.07, 2.23, 0.95, and 0.71, respectively. As the investigation encompassed a wide frequency range, including high frequencies, it was anticipated the average MOF values would be high. Comparing these values with the average loss damping factor, it becomes evident that the modal overlap factor in the experiments was primarily influenced by the loss damping factor, rather than the modal density. Hence, amongst the specimens, the composite sandwich exhibited the highest MOF due to its superior loss damping factor (e.g., see Ege et al. (2009); Denis et al. (2014) for more information on MOF and its interpretation).

Consequently, Figure 10 shows the measured SPL spectrum and ones simulated before and after the updating for the composite sandwich plate. In Figure 10, especially in the zoom window for the frequency range of 0 to 2000 Hz, it is evident that the updated simulation is more consistent with the actual measurement acquired by the microphone. In other words, these SPL results also indicate the ability of the updating approach in improving the calculation associated with the 6^{th} order problem of the sandwich panel.

Also, for the composite laminate specimen, similar vibroacoustic comparisons between the measurements and the simulated ones could be performed. Figures 11, and 12 show the comparisons corresponding to the average vibration field and the sound pressure level corresponding to the composite laminate panel, respectively. According to these figures, we can see the improvements in the simulations for both the vibration and the SPL after applying the updating procedures to the calculations. So, the vibration observations taken with the LDV system show how the RMS value of the simulation error in the state of applying the updating method compared to the state before applying the updating method has decreased

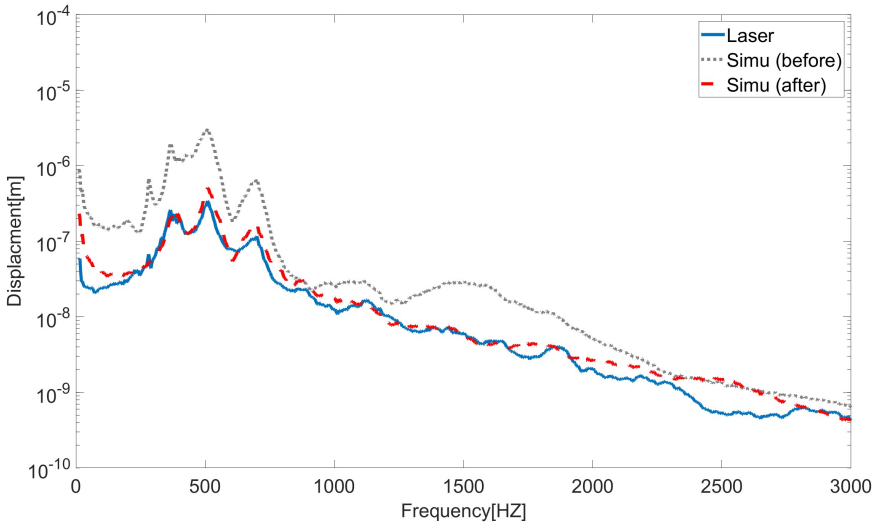

Figure 9: The average of the vibration field for the composite sandwich plate, measured by the LDV system (Laser), compared with the simulations done before and after the updating (Simu (before and after))

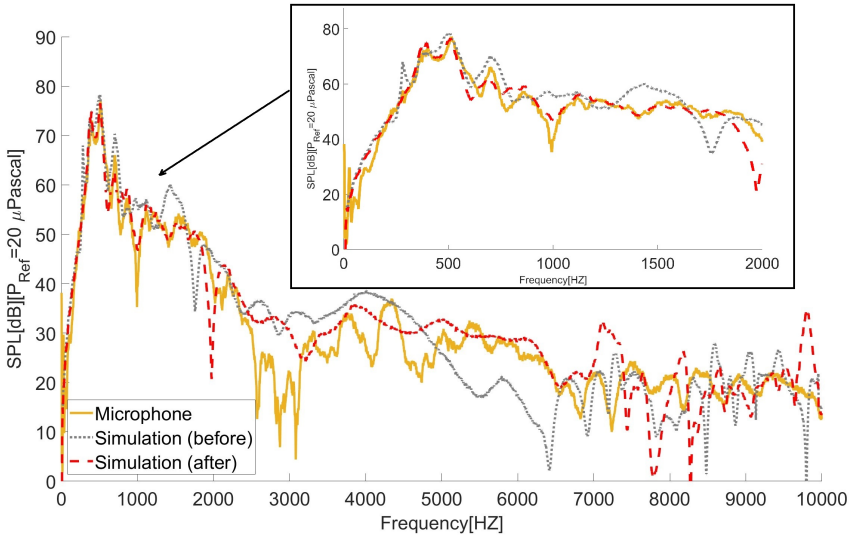

Figure 10: The SPL comparison corresponding to the composite sandwich plate, between the simulations (before and after updating) and microphone measurement; the small zoom window shows such SPL comparison for low frequencies

from a value of 3.37×10^{-7}m to a value of 1.16×10^{-7}m, which shows that the modeling and simulation of vibration field for the laminate panel have improved

by about 2.93 times from the point of view of the RMS errors.

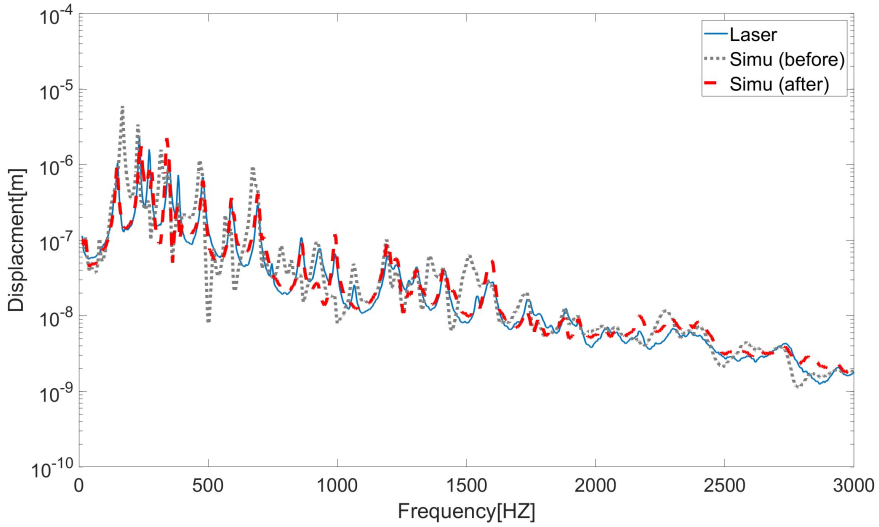

Figure 11: The average of the vibration field for the composite laminate plate, measured by the LDV system (Laser), compared with the simulations done before and after the updating (Simu (before and after))

Furthermore, for the other specimens, aluminium, and steel plates, we also carried out similar comparisons between the measurements and the simulated ones. As discussed before, the measurements associated with the aluminium and steel plates have been performed as extra validations for the updating procedures associated with the 4^{th} order problem (see Eq.(4)). Figures 13, and 15 have summarized the comparisons corresponding to the average vibration field over the aluminium, and steel plates, respectively, and also, Figures 14, and 16 illustrate the comparison of the SPL spectra for the frequency interval $[0, 1000]$Hz before and after the updating procedures. According to these figures, similar to the results of the composite panels (sandwich and laminate ones), we can see the enhancement in the simulations for both the vibration and the sound pressure levels. Based on the results obtained with the LDV (laser) system, the RMS of the simulation error in two states, before and after the updating, was obtained for the aluminum plate, respectively, 5.30×10^{-7}m and 1.19×10^{-7}m, and similarly, for the steel plate, the values of 1.45×10^{-6}m and 4.47×10^{-7}m were obtained, respectively. Therefore, this means that from the RMS point of view, the updating method has been able to enhance the modeling and simulation corresponding to the aluminum and steel plates by 4.46 and 3.25 times, respectively, which are actually the improvement to

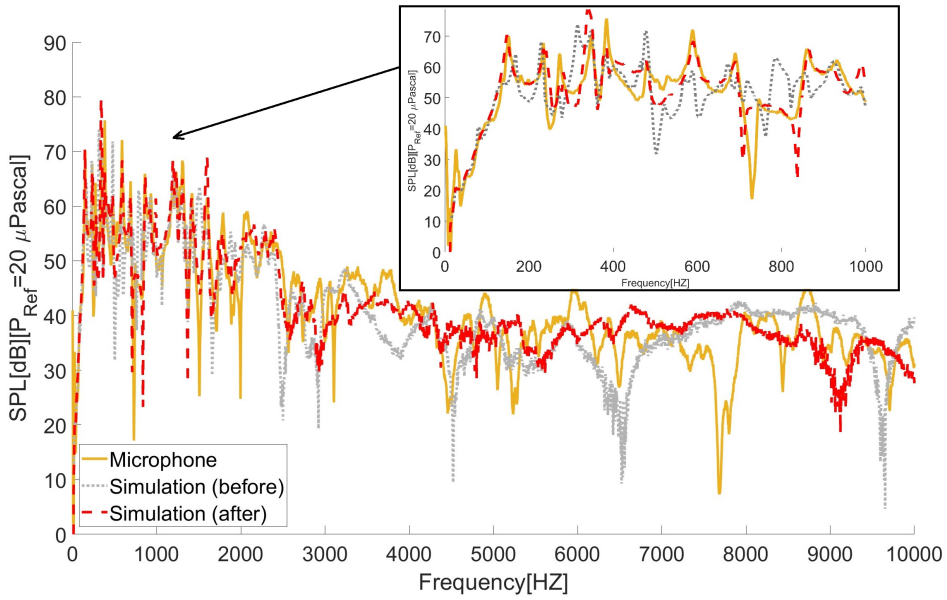

Figure 12: The SPL comparison corresponding to the composite laminate plate, between the simulations (before and after updating) and microphone measurement; the small zoom window shows such SPL comparison for low frequencies

the model of the 4^{th} order problem.

4.6 Discussion of results

The results were also consistent with previous research in which almost similar case studies were conducted. For example, in the numerical calculations, in order to preliminarily have the mechanical properties of the composite sandwich and laminate specimens, the characteristics of the CFRP ply with epoxy matrix as well as the Nomex core were extracted from some previous studies such as Shahdin et al. (2011); Qi et al. (2019); Zhou et al. (2021); Adams and Maheri (1993); Zhou et al. (2021) (see Section 4.2). Then, at each stage, the calculated parameters were compared with these preliminary values. Of course, the final updated parameters, while being close to such preliminary values, have also enhanced the vibroacoustic simulations. According to these results, the shear modulus of the Nomex core of the composite sandwich panel as one of the updated parameters was obtained at the IWC and final steps of the proposed hybrid approach, equal to 68MPa and 71MPa, respectively, which are close to the preliminary value obtained from the literature. Similarly, according to the previous studies on the mechanical properties

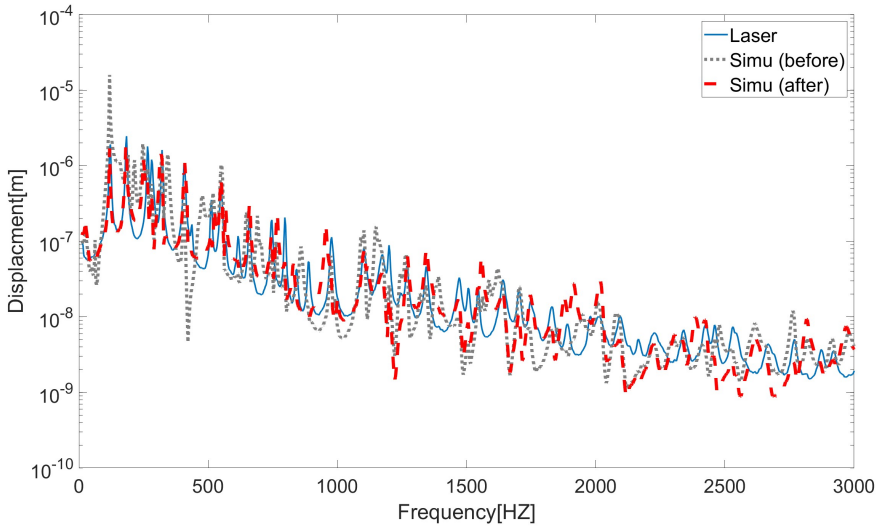

Figure 13: The average of the vibration field for the aluminium plate, measured by the LDV system (Laser), compared with the simulations done before and after the updating (Simu (before and after))

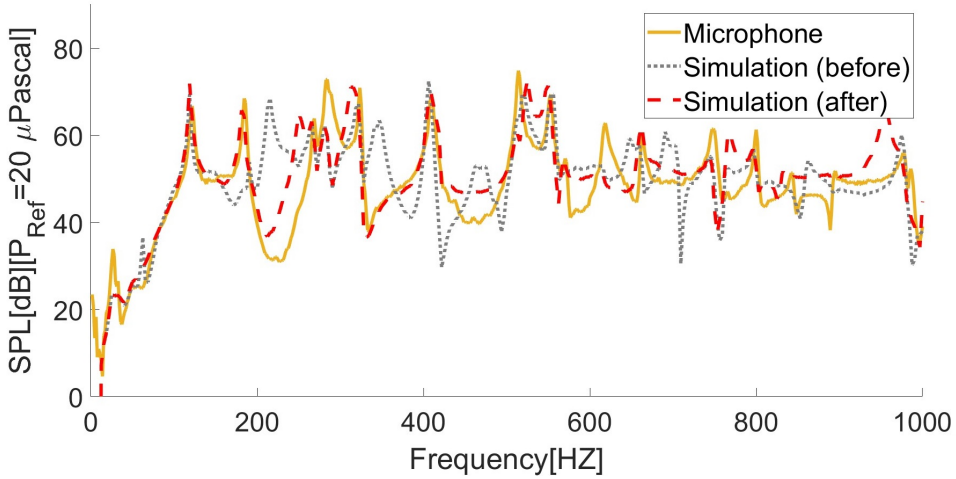

Figure 14: The SPL comparison corresponding to the aluminium plate, between the simulations (before and after updating) and microphone measurement

of the CFRP ply with epoxy matrix, at first, the bending stiffness coefficients corresponding to the composite laminate and sandwich panel, could also be initially assessed via the classical laminate theory. Then the bending stiffness coefficients,

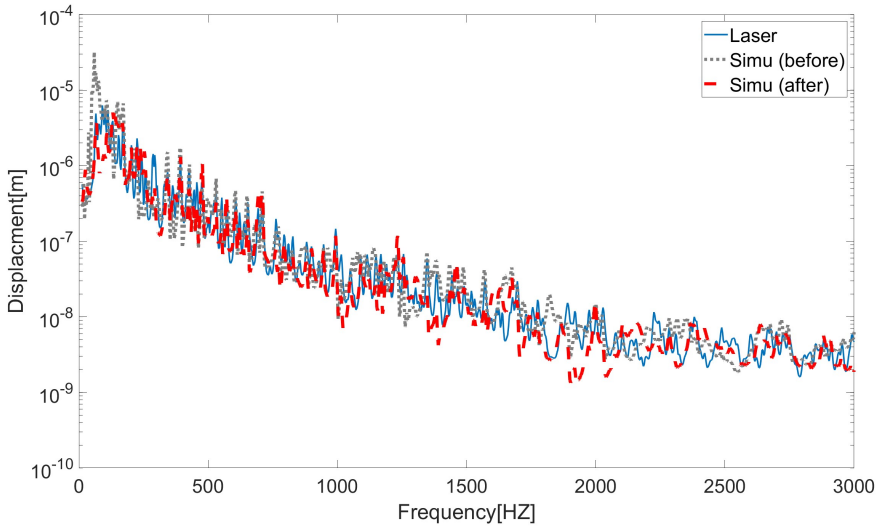

Figure 15: The average of the vibration field for the steel plate, measured by the LDV system (Laser), compared with the simulations done before and after the updating (Simu (before and after))

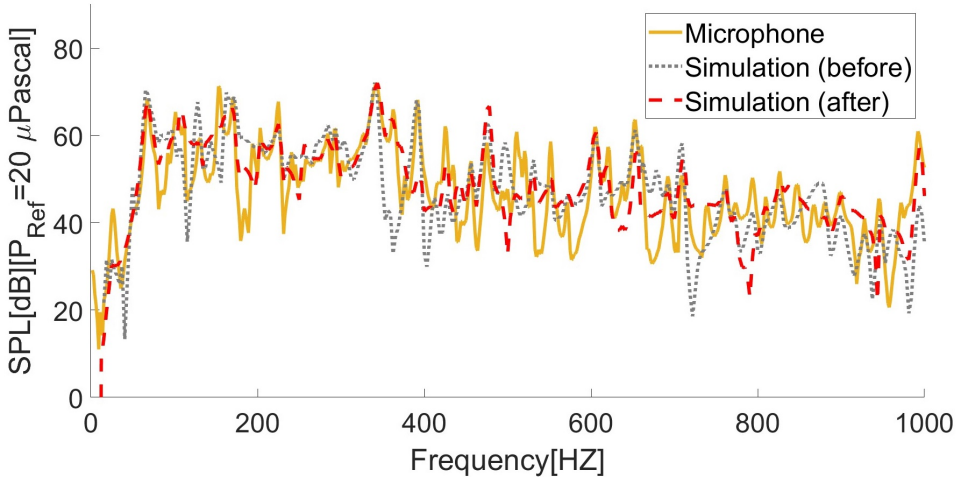

Figure 16: The SPL comparison corresponding to the steel plate, between the simulations (before and after updating) and microphone measurement

obtained at the IWC and final steps, were able to show their good agreement with such preliminary assessment (cf. Tables 2 to 4 in Section 4).

5 Conclusions

This study aimed to develop a hybrid updating approach adapted for the 4^{th} and 6^{th} order problems, required for the vibroacoustic modeling of composite panels. This approach is based on the hierarchical functions for analytically formulating the problems, IWC technique for the initial identification of parameters, and least squares optimizations including Baruch and total least squares method for updating models and parameters. The approach utilizes the IWC method, employing the 4^{th} and 6^{th} order dispersion relations for parameter identification. It follows the model updating process via the Baruch method, which is fed with the parameters identified by the IWC. The hierarchical functions provide the models with analytical formulations facilitating the Baruch method, and the solutions provided by the Baruch method are used for finalizing the parameter updating process via the total least squares method. In fact, in the proposed hybrid approach, the methods are employed step by step, utilizing their respective capabilities in each stage to complement one another (see Section 3).

Herein, the main idea of the research was examined by laboratory experiments, including laser doppler vibrometry (LDV) measurements and sound recording for measuring spectra of sound pressure levels (SPL). The measurements were performed for some panels, including a composite sandwich panel, and a composite laminate one, as well as two isotropic plates for additional assessments. The efficiency of the method was attained through the progressive implementation of the proven capabilities of the aforementioned methods, where the progressive implementation facilitated the controlled evaluation of parameters, and avoided any time-consuming trial and error procedures. It was examined by different vibroacoustic comparisons between the measurements and the simulations enjoying updated parameters. The LDV measurements indicated the ability of the approach in enhancing the simulations for modeling the vibration field. Furthermore, the comparison associated with the measured SPL spectra could experimentally validate the accuracy of the simulated vibration. Such ability of the updating method in the precise modeling of the SPL can also be beneficial for the vibroacoustic modeling required in future psychoacoustic and perceptual assessments, which is one of the future goals of this research, too.

Moreover, the improvement of the Modal Assurance Criterion (MAC) can also be mentioned as one of the numerical achievements. As seen in Section 4.4, the proposed method could significantly enhance the cross Mac between the calculated and measured modes.

Accordingly, the study successfully attained a high level of agreement among all the collected data, which encompassed laboratory vibroacoustic measurements, mathematical simulations enhanced through updating procedures, and preliminary information on mechanical parameters. This consistency serves as evidence of the capabilities of the proposed hybrid approach for model and parameter updating, particularly in addressing 4th and 6th order problems, with a specific focus on thin and thick composite panels. These findings hold significant promise for conducting accurate simulations essential to the integrated vibroacoustic and psychoacoustic design of composite panels in future studies.

Acknowledgment

Financial supports of CeLyA (Lyon Acoustics Center, ANR-10-LABX-0060) are gratefully acknowledged. Also, we would like to express our thanks to Ms. Céline SANDIER, and Dr. Quentin LECLERE at the Laboratory of Vibration and Acoustics (LVA) of INSA for their assistance in performing LDV measurements. Moreover, we would like to extend our sincere gratitude to the editor and reviewers for dedicating their valuable time to enhancing our research.

CRediT authorship contribution statement

Y. AllahTavakoli: Conceptualization, Methodology, Laboratory experiments, Simulations, Software, Validation, Investigation, Writing – original draft. **M.N. Ichchou:** Conceptualization, Methodology, Supervision, Validation, Investigation, Writing – review and editing. **C. Marquis-Favre:** Conceptualization, Supervision, Validation, Investigation, Writing – review and editing. **N. Hamzaoui:** Conceptualization, Methodology, Laboratory experiments, Supervision, Validation, Investigation, Writing – review and editing.

Declaration of Competing Interest

The authors declare that they have no known competing financial interests or personal relationships that could have appeared to influence the work reported in this paper.

Data availability

Data will be made available on request.

References

Adams, R. and Maheri, M. (1993). The dynamic shear properties of structural honeycomb materials. *Composites Science and Technology*, 47(1):15–23.

Adams, R. A. and Fournier, J. J. (2003). *Sobolev spaces*. Elsevier.

Alvelid, M. (2013). Sixth order differential equation for sandwich beam deflection including transverse shear. *Composite Structures*, 102:29–37.

Baruch, M. (1978). Optimization procedure to correct stiffness and flexibility matrices using vibration tests. *AIAA Journal*, 16(11):1208–1210.

Berthaut, J., Ichchou, M., and Jezequel, L. (2005). K-space identification of apparent structural behaviour. *Journal of Sound and Vibration*, 280(3-5):1125–1131.

Beslin, O. and Nicolas, J. (1997). A hierarchical functions set for predicting very high order plate bending modes with any boundary conditions. *Journal of Sound and Vibration*, 202(5):633–655.

Brandt, A. (2011). *Noise and vibration analysis: signal analysis and experimental procedures*. John Wiley & Sons.

Carden, E. P. and Fanning, P. (2004). Vibration based condition monitoring: a review. *Structural Health Monitoring*, 3(4):355–377.

Chen, C., Duhamel, D., and Soize, C. (2006). Probabilistic approach for model and data uncertainties and its experimental identification in structural dynamics: Case of composite sandwich panels. *Journal of Sound and Vibration*, 294(1-2):64–81.

Chengwei, F., Haotian, L., Liem, R. P., Yatsze, C., and Lei, H. (2022). Hierarchical model updating strategy of complex assembled structures with uncorrelated dynamic modes. *Chinese Journal of Aeronautics*, 35(3):281–296.

Cherif, R., Chazot, J.-D., and Atalla, N. (2015). Damping loss factor estimation of two-dimensional orthotropic structures from a displacement field measurement. *Journal of Sound and Vibration*, 356:61–71.

Chronopoulos, D., Troclet, B., Bareille, O., and Ichchou, M. (2013). Modeling the response of composite panels by a dynamic stiffness approach. *Composite Structures*, 96:111–120.

Cuadrado, M., Artero-Guerrero, J., Pernas-Sánchez, J., and Varas, D. (2019). Model updating of uncertain parameters of carbon/epoxy composite plates from experimental modal data. *Journal of Sound and Vibration*, 455:380–401.

Daniel, I. M., Ishai, O., Daniel, I. M., and Daniel, I. (2006). *Engineering mechanics of composite materials*, volume 1994. Oxford University Press New York.

De Albuquerque, V. H. C., Tavares, J. M. R., and Durão, L. M. (2010). Evaluation of delamination damage on composite plates using an artificial neural network for the radiographic image analysis. *Journal of Composite Materials*, 44(9):1139–1159.

Denis, V., Pelat, A., Gautier, F., and Elie, B. (2014). Modal overlap factor of a beam with an acoustic black hole termination. *Journal of Sound and Vibration*, 333(12):2475–2488.

Droz, C., Bareille, O., and Ichchou, M. N. (2017). A new procedure for the determination of structural characteristics of sandwich plates in medium frequencies. *Composites Part B: Engineering*, 112:103–111.

Ege, K., Boutillon, X., and David, B. (2009). High-resolution modal analysis. *Journal of Sound and Vibration*, 325(4-5):852–869.

Esfandiari, A. (2014). Structural model updating using incomplete transfer function of strain data. *Journal of Sound and Vibration*, 333(16):3657–3670.

Fahy, F. J. (2000). *Foundations of engineering acoustics*. Elsevier.

Fan, J. and Njuguna, J. (2016). An introduction to lightweight composite materials and their use in transport structures. In *Lightweight Composite Structures in Transport*, pages 3–34. Elsevier.

Farrar, C. R., Doebling, S. W., and Nix, D. A. (2001). Vibration–based structural damage identification. *Philosophical Transactions of the Royal Society of London. Series A: Mathematical, Physical and Engineering Sciences*, 359(1778):131–149.

Friswell, M. and Mottershead, J. E. (1995). *Finite element model updating in structural dynamics*, volume 38. Springer Science & Business Media.

Friswell, M. I. (1990). *Updating finite element models using measured vibration data*. PhD thesis, Aston University.

Ghinet, S. and Atalla, N. (2011). Modeling thick composite laminate and sandwich structures with linear viscoelastic damping. *Computers & Structures*, 89(15-16):1547–1561.

Girardi, M., Padovani, C., Pellegrini, D., and Robol, L. (2021). A finite element model updating method based on global optimization. *Mechanical Systems and Signal Processing*, 152:107372.

Giurgiutiu, V. (2015). In *Structural health monitoring of aerospace composites*, pages 1–23. Academic Press, Oxford.

He, J. and Fu, Z.-F. (2001). 9 - modal analysis methods – time domain. In He, J. and Fu, Z.-F., editors, *Modal Analysis*, pages 180–197. Butterworth-Heinemann, Oxford.

Heylen, W., Lammens, S., Sas, P., et al. (1997). *Modal analysis theory and testing*, volume 200. Katholieke Universiteit Leuven Leuven, Belgium.

Humbert, L. (1999). *Recalage des modèles éléments finis à partir de mesures vibratoires*. PhD thesis, Ecully, Ecole centrale de Lyon.

Hwang, S.-F. and He, R.-S. (2006). A hybrid real-parameter genetic algorithm for function optimization. *Advanced Engineering Informatics*, 20(1):7–21.

Ichchou, M., Bareille, O., and Berthaut, J. (2008). Identification of effective sandwich structural properties via an inverse wave approach. *Engineering Structures*, 30(10):2591–2604.

Jaouen, L., Brouard, B., Atalla, N., and Langlois, C. (2005). A simplified numerical model for a plate backed by a thin foam layer in the low frequency range. *Journal of Sound and Vibration*, 280(3-5):681–698.

Jones, R. M. (1999). *Mechanics of Composite Materials (2nd edition)*. CRC press.

Jones, R. M. (2018). *Mechanics of composite materials*. CRC press.

Katunin, A. and Przystałka, P. (2014). Damage assessment in composite plates using fractional wavelet transform of modal shapes with optimized selection of spatial wavelets. *Engineering Applications of Artificial Intelligence*, 30:73–85.

Kaw, A. K. (2005). *Mechanics of composite materials*. CRC press.

Kerschen, G., Worden, K., Vakakis, A. F., and Golinval, J.-C. (2006). Past, present and future of nonlinear system identification in structural dynamics. *Mechanical Systems and Signal Processing*, 20(3):505–592.

Khatir, S., Tiachacht, S., Le Thanh, C., Ghandourah, E., Mirjalili, S., and Wahab, M. A. (2021). An improved artificial neural network using arithmetic optimization algorithm for damage assessment in fgm composite plates. *Composite Structures*, 273:114287.

Kohsaka, K., Ushijima, K., and Cantwell, W. J. (2021). Study on vibration characteristics of sandwich beam with bcc lattice core. *Materials Science and Engineering: B*, 264:114986.

Lafont, T., Totaro, N., and Le Bot, A. (2014). Review of statistical energy analysis hypotheses in vibroacoustics. *Proceedings of the Royal Society A: Mathematical, Physical and Engineering Sciences*, 470(2162):20130515.

Le Bot, A. (2015). *Foundation of statistical energy analysis in vibroacoustics*. OUP Oxford.

Lesueur, C. and Nicolas, J. (1989). In *Rayonnement acoustique des structures (Acoustic Radiation of Structures)*. Acoustical Society of America.

Li, J. and Narita, Y. (2013). Analysis and optimal design for the damping property of laminated viscoelastic plates under general edge conditions. *Composites Part B: Engineering*, 45(1):972–980.

Lyon, R. H., DeJong, R. G., and Heckl, M. (1995). In *Theory and application of statistical energy analysis*. Acoustical Society of America.

Markovsky, I. and Van Huffel, S. (2007). Overview of total least-squares methods. *Signal processing*, 87(10):2283–2302.

McDaniel, J. G., Dupont, P., and Salvino, L. (2000). A wave approach to estimating frequency-dependent damping under transient loading. *Journal of Sound and Vibration*, 231(2):433–449.

McDaniel, J. G. and Shepard Jr, W. S. (2000). Estimation of structural wave numbers from spatially sparse response measurements. *The Journal of the Acoustical Society of America*, 108(4):1674–1682.

Mead, D. and Markus, S. (1969). The forced vibration of a three-layer, damped sandwich beam with arbitrary boundary conditions. *Journal of Sound and Vibration*, 10(2):163–175.

Mottershead, J. E. and Friswell, M. (1993). Model updating in structural dynamics: a survey. *Journal of Sound and Vibration*, 167(2):347–375.

Mottershead, J. E., Link, M., and Friswell, M. I. (2011). The sensitivity method in finite element model updating: A tutorial. *Mechanical Systems and Signal Processing*, 25(7):2275–2296.

Mrazova, M. (2013). Advanced composite materials of the future in aerospace industry. *INCAS Bulletin*, 5(3):139.

Narayanan, S. and Shanbhag, R. (1981). Sound transmission through elastically supported sandwich panels into a rectangular enclosure. *Journal of Sound Vibration*, 77(2):251–270.

Narayanan, S. and Shanbhag, R. (1982). Sound transmission through a damped sandwich panel. *Journal of Sound and Vibration*, 80(3):315–327.

Nilsson, E. and Nilsson, A. (2002). Prediction and measurement of some dynamic properties of sandwich structures with honeycomb and foam cores. *Journal of Sound and Vibration*, 251(3):409–430.

Ozdemir, A. A. and Gumussoy, S. (2017). Transfer function estimation in system identification toolbox via vector fitting. *IFAC-PapersOnLine*, 50(1):6232–6237.

Petrone, G. and Meruane, V. (2017). Mechanical properties updating of a non-uniform natural fibre composite panel by means of a parallel genetic algorithm. *Composites Part A: Applied Science and Manufacturing*, 94:226–233.

Qi, Z., Liu, Y., and Chen, W. (2019). An approach to predict the mechanical properties of cfrp based on cross-scale simulation. *Composite Structures*, 210:339–347.

Roy, R., Park, S.-J., Kweon, J.-H., and Choi, J.-H. (2014). Characterization of nomex honeycomb core constituent material mechanical properties. *Composite Structures*, 117:255–266.

Sarlin, E., Liu, Y., Vippola, M., Zogg, M., Ermanni, P., Vuorinen, J., and Lepistö, T. (2012). Vibration damping properties of steel/rubber/composite hybrid structures. *Composite Structures*, 94(11):3327–3335.

Shahdin, A., Morlier, J., Mezeix, L., Bouvet, C., and Gourinat, Y. (2011). Evaluation of the impact resistance of various composite sandwich beams by vibration tests. *Shock and Vibration*, 18(6):789–805.

Sinha, J. K., Friswell, M., and Edwards, S. (2002). Simplified models for the location of cracks in beam structures using measured vibration data. *Journal of Sound and Vibration*, 251(1):13–38.

Stanbridge, A. B., Martarelli, M., and Ewins, D. J. (2004). Measuring area vibration mode shapes with a continuous-scan ldv. *Measurement*, 35(2):181–189.

Standoli, G., Giordano, E., Milani, G., and Clementi, F. (2021). Model updating of historical belfries based on oma identification techniques. *International Journal of Architectural Heritage*, 15(1):132–156.

Tam, J. H., Ong, Z. C., and Ho, K. W. (2019). Composite material identification using a two-stage meta-heuristic hybrid approach incorporated with a two-level frf selection scheme. *Journal of Sound and Vibration*, 456:407–430.

Tsai, Y.-T., Pawar, S., and Huang, J. H. (2015). Optimizing material properties of composite plates for sound transmission problem. *Journal of Sound and Vibration*, 335:174–186.

Van Belle, L., Claeys, C., Deckers, E., and Desmet, W. (2017). On the impact of damping on the dispersion curves of a locally resonant metamaterial: Modelling and experimental validation. *Journal of Sound and Vibration*, 409:1–23.

Wang, J., Wang, C., and Zhao, J. (2017). Frequency response function-based model updating using kriging model. *Mechanical Systems and Signal Processing*, 87:218–228.

Wang, W., Mottershead, J. E., Ihle, A., Siebert, T., and Schubach, H. R. (2011). Finite element model updating from full-field vibration measurement using digital image correlation. *Journal of Sound and Vibration*, 330(8):1599–1620.

Zhou, Y., Liu, A., Xu, Y., Guo, Y., Yi, X., and Jia, Y. (2021). Frequency-dependent orthotropic damping properties of nomex honeycomb composites. *Thin-Walled Structures*, 160:107372.

Živanović, S., Pavic, A., and Reynolds, P. (2005). Vibration serviceability of footbridges under human-induced excitation: a literature review. *Journal of Sound and Vibration*, 279(1-2):1–74.